Capillary Electrophoretic Analysis Based on the Formation of Heteropolyoxomolybdates

中島，陽一

(Degree)
博士（理学）

(Date of Degree)
2001-03-31

(Date of Publication)
2009-07-21

(Resource Type)
doctoral thesis

(Report Number)
甲2248

(URL)
https://hdl.handle.net/20.500.14094/D1002248

博 士 論 文

Capillary Electrophoretic Analysis Based on the Formation of Heteropolyoxomolybdates

（ヘテロポリオキソモリブデート錯体生成に基づくキャピラリー電気泳動分析）

平成13年1月

神戸大学大学院自然科学研究科

中島　陽一

Contents

Chapter 1

Introduction

A lot of chemical species exist in the environment. Particularly, all sorts of the ionic species exist as aquo-complexes and organic or inorganic complexes, and several ionic species have plural oxidational states. The ionic species according to the existing states, have different effects on ecological systems and cycles of nature. From this point of view, the separation chemistry has played an important part in natural science. The study of separation and determination of each species, the so-called 'speciation' is the fundamentals of the geochemical, environmental and biological variability of elements in natural systems [1–3].

The capillary electrophoretic analysis (CE), which is originated by Jorgenson and Lukacs [4], has been widely used for ion analysis and/or separation due to high separation efficiencies and simple equipment in recent years (for reviews see, eg., [5–7]). CE has shown considerable promise in the separation and analysis of biological and environmental samples [8]. The conventional CE system is equipped with a high

voltage DC power supply, a simple UV-visible detector and a data collecting system (Fig. 1.1). A photo diode array UV-visible detector instead of a simple UV-visible detector is furnished with the latest system. In CE analysis, the application of an electric field across an electrolyte-filled capillary induces the migration of solutes. The electrophoretic mobility of each solute is a function of the charge and hydrodynamic radius of the solute as well as the viscosity of the electrolyte. As a result, small differences in the charge-to-size ratio of solutes can lead to spatial separation. CE possesses several advantages that make it a powerful technique for analyzing biological and environmental mixtures. Very small volumes (nL order) of an impure sample can be analyzed, and separation can be conducted in aqueous solution under environmentally and biologically relevant pH and ionic strength conditions. In addition to its use as a separation tool, fundamental binding information is also accessible using CE including oxidation state, stoichiometry, and binding constant determinations [9,10].

In general, inorganic ions are determined by indirect photometric detection [11], where the analyte ions replace a UV-absorbing organic or inorganic ion such as chromate, imidazole and so on. Despite many advantages, indirect photometric detection has the noisy baselines and the low sensitivity. As analytes can form large optical density substance, this permits the more sensitive determination of a lot of ions and the needless of more apparatus. Several metal ions are converted into complexes, most of all chelates, with high molar absorptivities of which more sensitive direct UV detection can be performed [12,13].

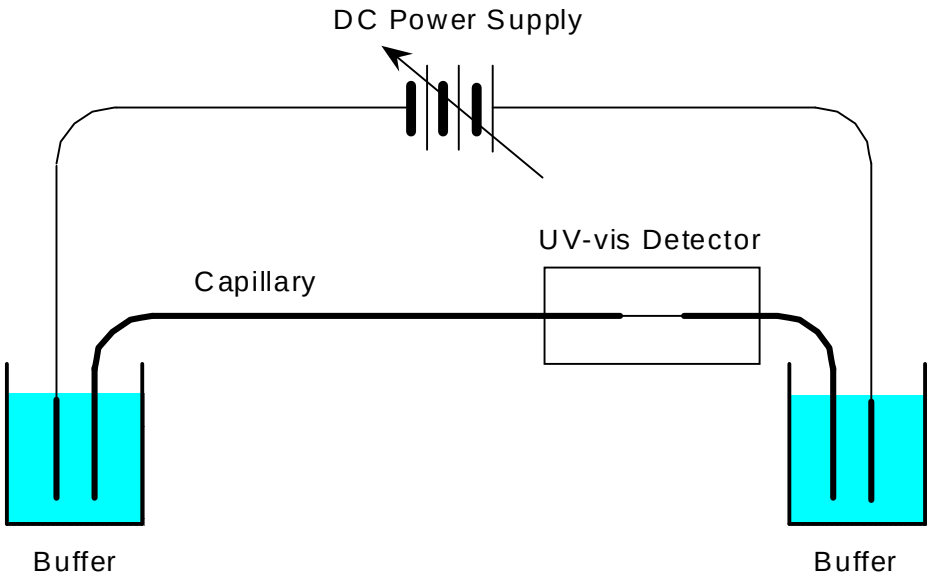

Figure 1.1: Schematic representation of capillary electrophoresis.

There are several reports of direct UV determination of anions [14], but the complexes incorporating anions have underutilized for determination of anions. Without any interaction between analytes and measurement systems, the CE method is quite different from high performance liquid chromatography. Therefore, there are many application study of the capillary electrophoretic analysis to chemical equilibrium [15]. The CE method also enables the speciation of chemical species to do, because the CE method has high separation-ability that identifies some ions independently.

Heteropolyoxomolybdates [16] have been used in industrial, medical, environmental fields and so on [17]. In particular, heterogeneous and homogeneous catalysts based upon the oxidation-reduction peculiarities of heteropolyoxomolybdates utilized for a wide variety of reactions [18,19]. And, there have been reports on the applications

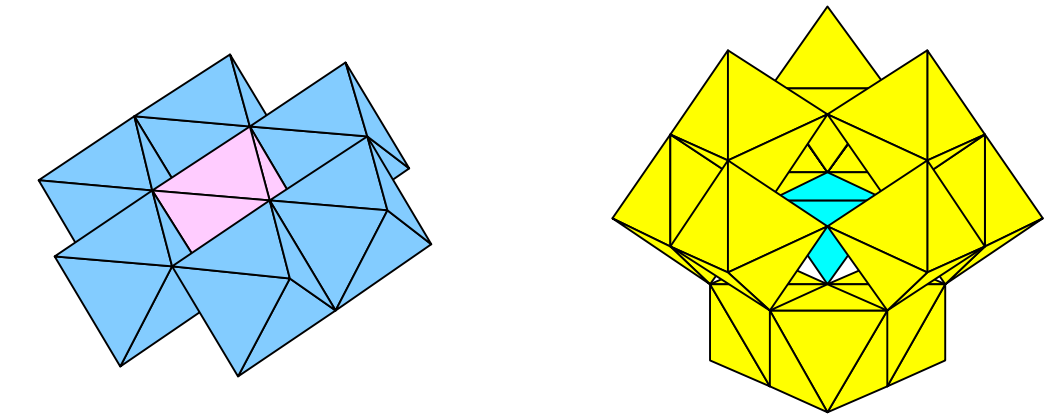

Figure 1.2: Typical Structures of Heteropolyoxomolybdates. (a) Anderson structure (XMo_6): X=I(VII), Cr(III), Al(III), Ga(III), Fe(III), Ni(II), Cu(II), Zn(II), Co(II). (b) Keggin structure (XMo_{12}): X=Si(IV), Ge(IV), P(V), As(V).

to pigments, ion-exchange materials and biochemistry. The formation of heteropolyoxomolybdates also has been applied widely to the spectrophotometric and voltammetric determination of various hetero-ions such as silicate, germanate, arsenate and phosphate (Fig. 1.2).

Heteropolyoxomolybdates that form predominantly always coexist with some minor species, and have many chemical equilibria in the solution. It is difficult to detect major and minor species independently with spectroscopic or electrochemical methods. Therefore, there are no applications for speciation except simultaneous voltammetric determination of V(IV) and V(V) [20] and simultaneous spectrophotometric determination of phosphate, phosphonate and diphosphate [21]. Hence the CE method among various heteropolyoxomolybdates can bring about novel knowledge of these complexes equilibria, but there

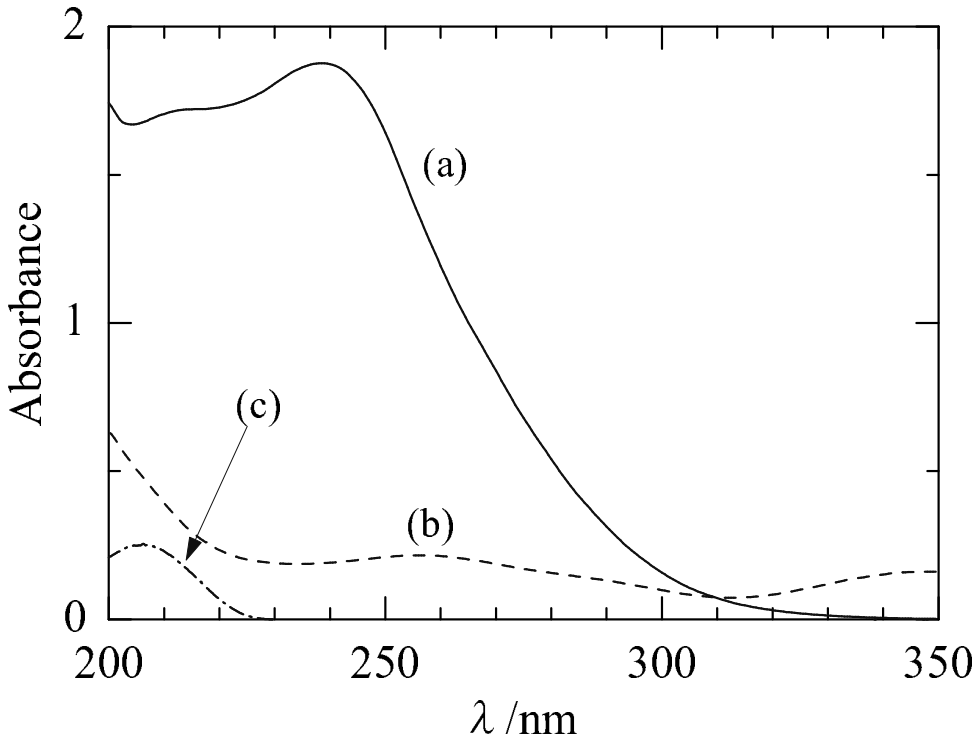

Figure 1.3: Absorption spectra for (a) 5×10^{-5} M $(NH_4)_3[CrMo_6O_{24}H_6]$ (pH 2.5), (b) 2.5×10^{-5} M $K_2Cr_2O_7$ (pH 2.5) and (c) 5×10^{-5} M imidazole (pH 4.0). Path length, 1cm.

are few investigations in point of this view [22]. On the other hand, since heteropolyoxomolybdates have larger optical densities than absorbing regents used for indirect UV detection, the sensitive CE analysis based on the formation of heteropolymolybdates is possible (Fig. 1.3).

In this study, the author has investigated the formation reaction of several heteropolyoxomolybdates at particular low concentrations of

Mo(VI) and hetero-ions, and the CE method has been applied to the determination of heteropolyoxomolybdates in solution.

In this dissertation, the author's contribution has been summarized in five chapters. In Chapter 2, UV-visible spectrophotometric studies have shown that the water-soluble anion ($[Cr^{III}Mo_6O_{24}H_6]^{3-}$) is formed at very low concentrations of Mo(VI) and Cr(III), and the complex-formation reaction proceeds rapidly even at ambient temperature. The simultaneous CE determination of Cr(III) and Cr(VI) which are oppositely charged in the form of Cr^{3+} and $Cr_2O_7{}^{2-}$ has been accomplished through the formation of a negatively charged complex, $[Cr^{III}Mo_6O_{24}H_6]^{3-}$. The complex formation reaction of Mo(VI)and I(VII) also has been studied by UV-visible spectroscopy, and has been applied to the CE determination of I(VII). On the basis of this studies, the author has described that the simultaneous CE determination of I(VII) and I(V) is possible because of the appearance of well defined two peaks corresponding to $[I^{VII}Mo_6O_{24}]^{5-}$ and $IO_3{}^-$ (Chapter 3).

In Chapter 4, the author has investigated the sample stacking effect to improve separation efficiency and detection limit of CE analysis based on the formation of heteropolyoxomolybdates. The field-amplified stacking has occurred by the reduction of buffer concentrations in sample solutions, and the transitional isotachophoretic stacking also has occurred by the addition of electrolysis in sample solutions . Owing to these stacking effects, the isomers of α- and β-Keggin-type dodecamolybdosilicates with approximately the same migration time could be separated satisfactorily, and the sensitivity for the determination of Cr(III) through the formation of hexamolybdo-

chromate(III)(3−) was improved.

In Chapter 5, the simultaneous determination of Ga(III) and Al(III) has been also possible, since the migration peaks due to the Anderson-type complexes become sensitive and well separated by mean of the sample stacking effect.

In Chapter 6, a sensitive method has been developed for the capillary electrophoretic determination of phosphate. The transitional isotachophoretic stacking also has been effective on the determination of phosphate based on the formation of a Keggin-type complex in aqueous-CH_3CN media. The quantity of phosphate in river water was determined by this capillary electrophoretic method and the results agreed with those obtained by the ion chromatographic and the colorimetric way.

Chapter 2

Simultaneous Determination of Cr(VI) and Cr(III)

2.1 Introduction

It is common knowledge that the Cr(VI) is more toxic than Cr(III) for the human organism, and the speciation of these compound is of importance [23]. In the usual method for the speciation of Cr(VI) and Cr(III), the Cr(VI) concentration is first determined spectrophotometrically at 540 nm as a complex with 1,5-diphenylcarbohydrazide (diphenylcarbazide) [24,25]. After the oxidation of Cr(III) to Cr(VI) with suitable oxidants, such as MnO_4^-, the total amount of Cr(VI) is determined again. Then, the Cr(III) concentration is estimated indirectly by subtracting the Cr(VI) concentration before oxidation from the total chromium concentration. The total amount of chromium can be determined as well by other methods, such as capillary electrophoresis [26,27], atomic absorption spectroscopy (at 357.9 nm) and inductively coupled argon plasma emission spectrometry (at 206.15

nm). In general, laborious procedures, including the oxidation of Cr(III) to Cr(VI), are needed to determine the respective concentrations of Cr(VI) and Cr(III) in the mixture.

Recently, ion chromatography has been widely used to determine separately the individual species of Cr(VI) and Cr(III) [28,29]. The separation is based on the fact that Cr(VI) and Cr(III) bear negative and positive charges, respectively; when one species is retained in the column, the other species passes through. A high-performance anion-exchange liquid chromatography was used to determine Cr(VI) and/or complexes of Cr(III) in biological samples [30]. Williams et al. have connected cation- and anion-exchange columns in parallel to determine simultaneously Cr(VI) and Cr(III) [31].

One can expect that the determination procedures may be improved by the conversion of cationic forms of Cr(III) into anionic forms through some complex- formation. In general, the complex-formation reaction proceeds very slowly, since Cr(III) is kinetically inert. The simultaneous determination of Cr(VI) and Cr(III) with capillary electrophoresis, which is used aminopolycarboxylic acids as the complex reagents, employed by several groups [32–34]. Jung et al., proposed a method based on the formation of an anionic complex of Cr(III) with EDTA [32]. In this case, it takes more than three days to complete the complex-formation reaction at room temperature; boiling of the reaction mixture is needed to accelerate the complex-formation reaction. New complexing reagents to react rapidly with Cr(III) are being eagerly searched in order to develop a simple electrophoretic method for the speciation of chromium.

Although a hexamolybdochromate(III)(3−) ($[CrMo_6O_{24}H_6]^{3-}$) has been prepared by boiling a reaction mixture of Mo(VI) and Cr(III) [35–38], its existence in solution remains to be confirmed. The UV-visible spectrophotometric studies have shown that the water-soluble $[CrMo_6O_{24}H_6]^{3-}$ anion is formed at very low concentrations of Mo(VI) and Cr(III), and the complex-formation reaction proceeds rapidly even at ambient temperature. On the other hand, no complex-formation reaction of Mo(VI) with Cr(VI) occurs. In the electropherogram, two peaks due to $Cr_2O_7{}^{2-}$ and $[CrMo_6O_{24}H_6]^{3-}$ were well separated, and the peak-areas were dependent linearly on the respective concentrations of Cr(III) and Cr(VI). This complex-formation reaction made it possible to develop a simple and sensitive method for the simultaneous determination of Cr(VI) and Cr(III) with capillary electrophoresis.

2.2 Experimental

2.2.1 Apparatus

Analyses were performed on an Otsuka Denshi Model CAPI–1000 capillary electrophoresis system equipped with a UV detector. The fused-silica capillaries used were 70 cm in length with an internal diameter of 75 μm. The distance from the point of injection to the detector was 50 cm. The solutes were injected for 2 s in the hydrodynamic mode. The electropherograms were collected with a Hitachi Model D–2500 chromato-integrator. UV-visible spectra were recorded on a Hitachi Model U–3000 spectrophotometer. The contents of molyb-

denum and chromium in the complex salt were determined with a Shimadzu Model ICPS–5000 inductively coupled argon plasma emission spectrometer. The NH_4^+ content was determined with a Hitachi ion chromatograph. The water content was determined with a Rigaku Denki Model TAS–100 thermal analyzer.

2.2.2 Reagents

All of the reagents were of analytical grade and were used as received. Standard solutions of Cr(VI) and Cr(III) were prepared by dissolving $K_2Cr_2O_7$ and $Cr(NO_3)_3 \cdot 9H_2O$ in distilled water, respectively.

2.2.3 Preparation of$(NH_4)_3[CrMo_6O_{24}H_6] \cdot 5H_2O$

The hexamolybdochromate(III)(3−) was isolated as the NH_4^+ salt to characterize it. When the pH of a 100 ml solution containing 2.4 g of $Na_2MoO_4 \cdot 2H_2O$ and 0.40 g of $Cr(NO_3)_3 \cdot 9H_2O$ was adjusted to 2.5 with HCl, a pink solution was obtained, indicating the formation of the desired complex anion. The addition of 10.7 g of NH_4Cl yielded a pink precipitate, which was collected by filtration, washed with water and ethanol, and air-dried. The precipitate was further purified by recrystallization from a 10% (v/v) ethanol-water solution. Anal. Calcd for $(NH_4)_3[CrMo_6O_{24}H_6] \cdot 5H_2O$: Mo, 49.54; Cr, 4.48; NH_4^+, 4.66; H_2O, 12.4%. Found: Mo, 49.86; Cr, 4.48; NH_4^+, 4.90; H_2O, 12.5%. IR (1000–400 cm^{-1}): 945, 926, 895, 656, 579, 554, 415 cm^{-1} (Fig. 2.1).

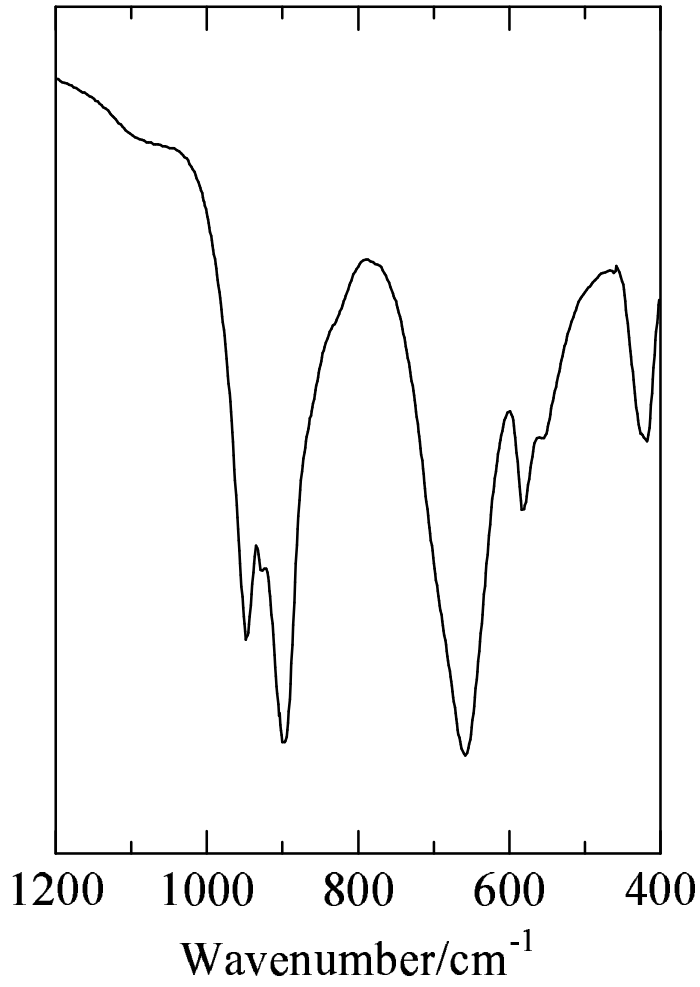

Figure 2.1: An IR spectrum of $(NH_4)_3[CrMo_6O_{24}H_6]\cdot 5H_2O$ in a KBr pellet.

2.3 Results and Discussion

2.3.1 Formation of the $[CrMo_6O_{24}H_6]^{3-}$ anion in aqueous solution

Figure 2.2 shows the absorption spectra for 3×10^{-4} M Mo(VI), 5×10^{-5} M Cr(III) and a mixture of 3×10^{-4} M Mo(VI) + 5×10^{-5} M Cr(III) in an aqueous solution of pH 2.0. As shown in Fig. 2.2(c), the solution of Mo(VI) and Cr(III) showed a spectrum entirely different from the solution containing only each component. At wave-lengths of 240–320 nm, the absorbance values for the mixture were greater than those expected from a simple additivity of the absorbance values of Mo(VI) and Cr(III), indicating the formation of a heteropoly complex.

In order to study the compositional ratio of Mo/Cr in the heteropoly anion, the mole-ratio method was applied by varying the Cr(III) concentration at a constant Mo(VI) concentration of 1.0 mM and by varying the Mo(VI) concentration at a constant Cr(III) concentration of 0.2 mM. In both procedures, the results indicate a Mo/Cr ratio of 6/1. This confirms that the $[CrMo_6O_{24}H_6]^{3-}$ complex is formed even in such low concentrations of Mo(VI) and Cr(III). It must be noted that the $[CrMo_6O_{24}H_6]^{3-}$ complex is formed immediately upon mixing Mo(VI) and Cr(III) solutions at pH values of 2–3, and that it is stable for at least one week.

The absorption spectrum of 2×10^{-4} M $Cr_2O_7{}^{2-}$ at pH 2.0 is also shown in Fig. 2.2(d). The $Cr_2O_7{}^{2-}$ solution shows an absorption maximum at 256 nm. It should be noted that no complex formation of Cr(VI) with Mo(VI) occurs. On the basis of the absorption spectra,

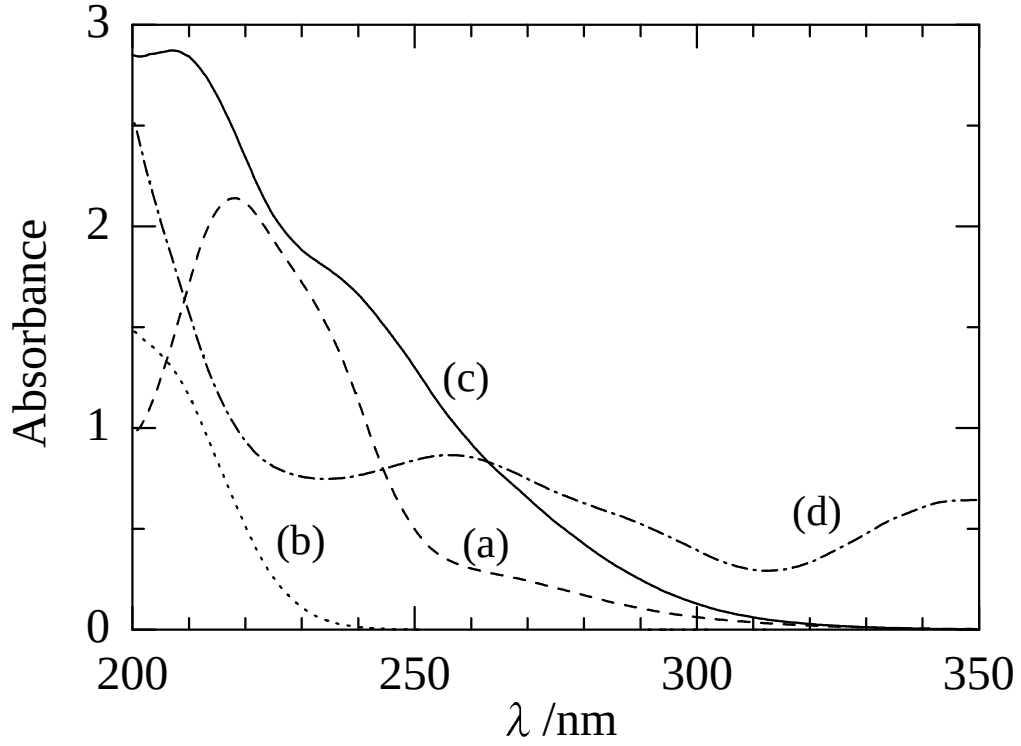

Figure 2.2: Absorption spectra for (a) 3×10^{-4} M Mo(VI), (b) 5×10^{-5} M Cr(III), (c) a mixture of 3×10^{-4} M Mo(VI)+5×10^{-5} M Cr(III) and (d) 2×10^{-4} M $Cr_2O_7^{2-}$ in an aqueous solution (pH 2.0). Path length, 1 cm.

a wavelength of 256 nm was chosen as optimum for the detection of Cr(III) and Cr(VI).

2.3.2 Effect of the Mo(VI) concentration on the electropherogram

In order to optimize the Mo(VI) concentration in a sample solution to be determined, test solutions were prepared by varying the Mo(VI) concentration (1×10^{-3}–1×10^{-2} M) while keeping a concentration of

Cr(III) and Cr(VI) equal 5×10^{-5} M in a 0.1 M monochloroacetate buffer (pH 2.0). The test solutions were introduced into the capillary and electropherograms were recorded. In a series of electrophoretic measurements, a 0.1 M monochloroacetate buffer (pH 2.0) was also used as a migration buffer. At Mo(VI) concentrations $\geqq 5\times10^{-3}$ M, the peaks for both the Cr(III) and Cr(VI) species split into two or more components, although the behavior could not be fully explained at present. With Cr(III) concentrations $\leqq 1\times10^{-4}$ M, the optimum concentration of Mo(VI) was found to be 1×10^{-3} M. The increase in the Mo(VI) concentration only caused the linear range between the Cr(III) concentration and the peak-area to expand to higher Cr(III) concentrations.

2.3.3 Effect of the pH of the migration buffer

In the following, a test solution containing 5×10^{-5} M Cr(VI), 5×10^{-5} M Cr(III), 1×10^{-3} M Mo(VI) and 0.1 M monochloroacetate buffer (pH 2.0) was used to optimize various conditions for the capillary electrophoretic separation of Cr(III) and Cr(VI).

Preliminary experiments have shown that a proper choice of a migration buffer is important for the separation of Cr(III) and Cr(VI). Tartarate, formate, acetate and monochloroacetate buffer solutions of pH 2–4 were examined, and the best separation and peak-shape were obtained using a 0.1 M monochloroacetate buffer as the migration buffer. The effect of the buffer pH on the electropherogram is shown in Fig. 2.3. At pH 2.0 (Fig. 2.3(a)), the first peak is due

to $Cr_2O_7^{2-}$ and the second is due to the $[CrMo_6O_{24}H_6]^{3-}$ anion; no peaks due to free isopolymolybdate species were observed within 10 min. Both peak-areas were plotted against the pH, and are shown in Fig. 2.4. In the pH range 2–3.5, both species showed well-shaped peaks. At pH values > 3.5, however, free isopolymolybdate species existing in an excess amount migrated faster than the Cr(VI) and Cr(III) species, and peaks for Mo(VI), Cr(III) and Cr(VI) species sometimes overlapped (Fig. 2.3(c)). In general, isopolymolybdate species continuously change with the variation of the pH values in aqueous solution [39]. These behaviors can be accounted for in terms of the increase of the negative charge per molybdenum in isopolymolybdate species. Simultaneously, the baseline became noisy as the pH was increased. In conclusion, a buffer pH of 2.0 was chosen as being optimum, because the electropherogram showed sharp and reproducible peaks for both Cr(III) and Cr(VI) species and a smooth baseline.

2.3.4 Effect of the temperature in a capillary system

After standing for some period at room temperature, the test solution was introduced into a capillary thermostated at 30 or 45°C; the period is denoted as the reaction time. The peak-areas for both chromium species were measured as a function of the reaction time, and are shown in Fig. 2.5. The peak-areas for the Cr(VI) species were not affected by the variation in the reaction time and the temperature. On the other hand, the peak-area for the Cr(III) species grew with the reaction time at a temperature of 30°C, and attained a constant

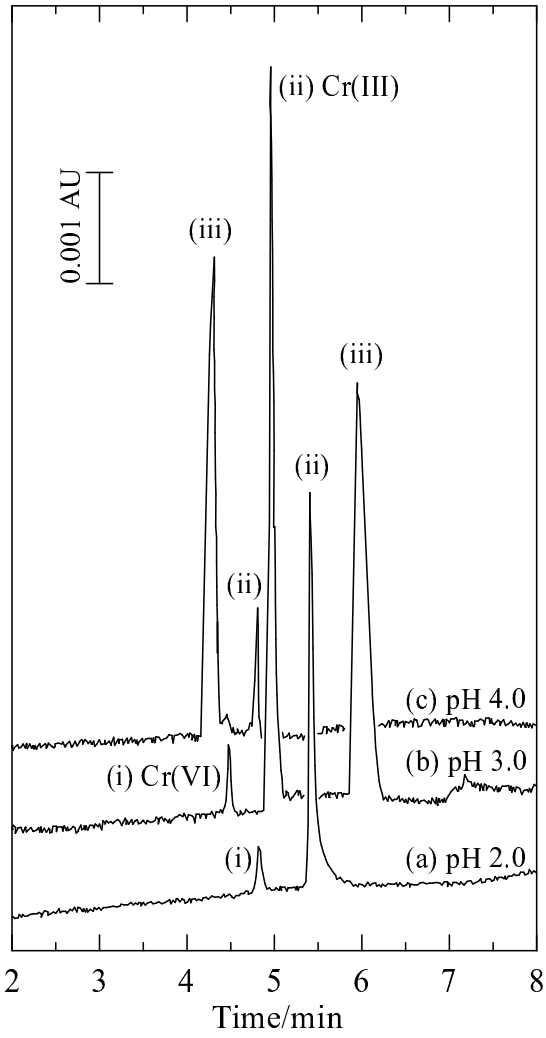

Figure 2.3: Electropherograms for a test solution containing 5×10^{-5} M Cr(VI), 5×10^{-5} M Cr(III), 1×10^{-3} M Mo(VI) and 0.1 M monochloroacetate buffer (pH 2.0). pH values of the migration buffer (0.1 M monochloroacetate): (a) 2.0; (b) 3.0; (c) 4.0. (i) Cr(VI); (ii) Cr(III); (iii) Mo(VI). Applied voltage; −20.0 kV.

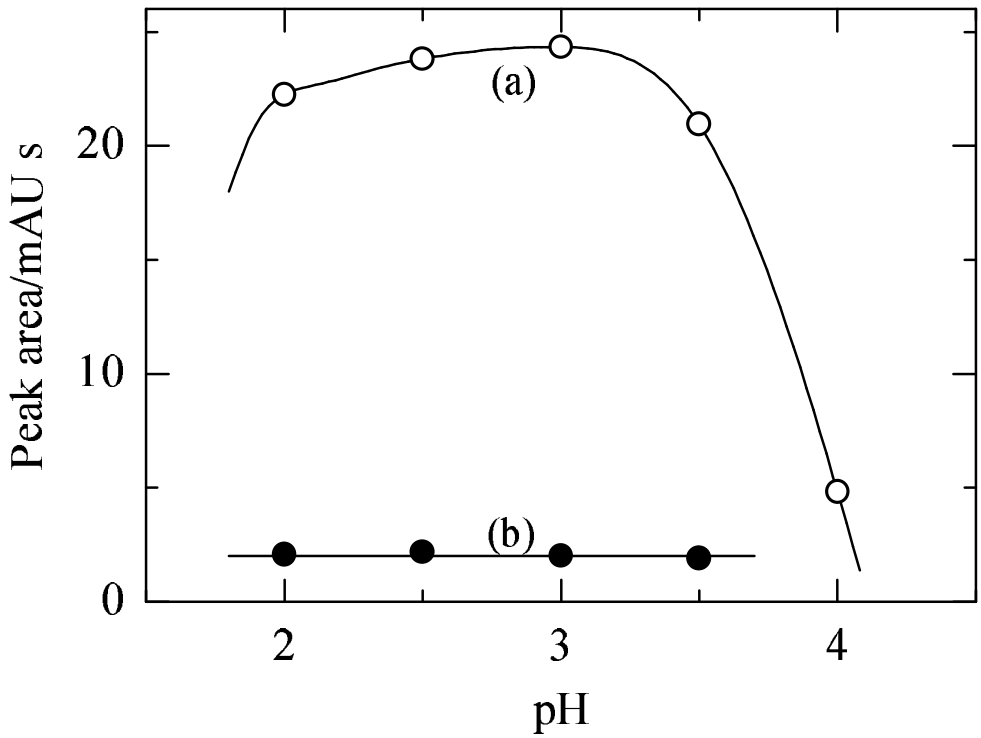

Figure 2.4: Relationship between the pH values of the migration buffer and the peak-areas for (a) Cr(III) and (b) Cr(VI). The test solution was the same as in Fig. 2.3.

value at a reaction time of 20 min. At a temperature of 45°C, however, the peak-area was independent of the reaction time. The temperature of the capillary system was set at 45°C, because reproducible results were obtained even when the test solution was introduced immediately after the preparation.

On the basis of these findings, calibration curves were obtained in the presence of 1×10^{-3} M Mo(VI) and 0.1 M monochloroacetate buffer (pH 2.0). The peak-areas showed linear dependencies on the

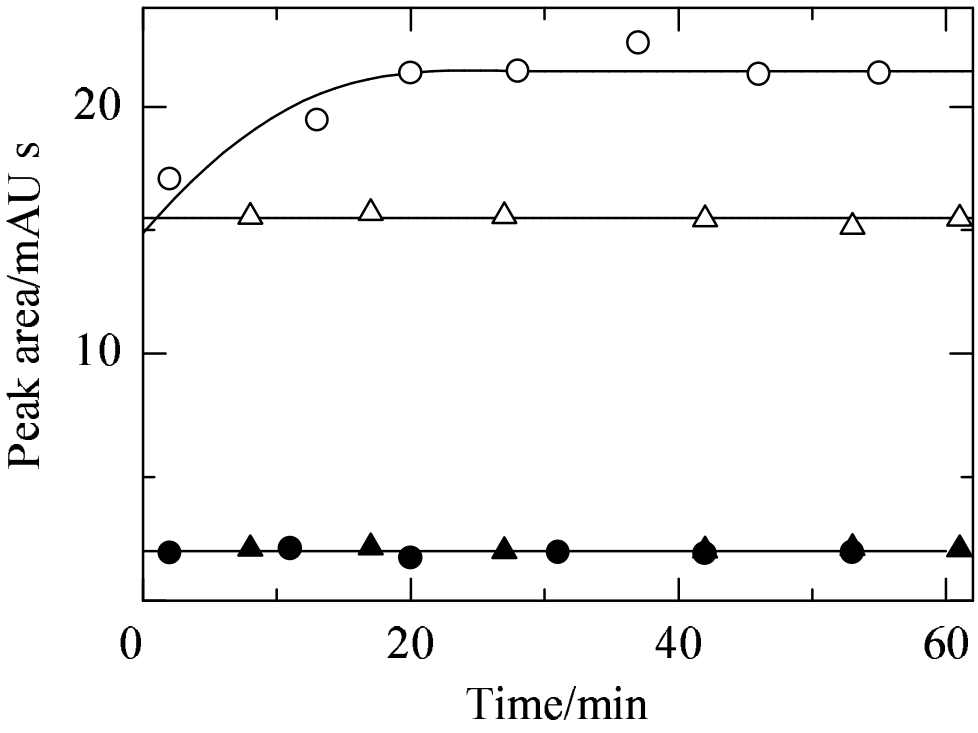

Figure 2.5: Peak-areas as a function of the reaction time at temperatures of (white and black circles); 30 and (white and black triangles); 40°C. (white circle and triangle); for Cr(III), (black circle and triangle); for Cr(VI). The test solution was the same as in Fig. 2.3. The migration buffer, 0.1 M monochloroacetate (pH 2.0).

concentrations of Cr(III) and Cr(VI) in the range of 5×10^{-6}–1×10^{-4} M and of 1×10^{-5}–1×10^{-4} M, respectively (Fig. 2.6).

2.3.5 Recommended procedure

Before sample injection, the capillary was filled with 0.1 M monochloroacetate buffer (pH 2.0). A 4 ml of 0.5 M monochloroacetate buffer (pH 2.0) was placed in a 20 ml volumetric flask. An appropriate amount of a sample solution was added after the addition of 2 ml of 10 mM Mo(VI), and the solution was diluted to the mark with distilled water. The analysis was carried out by simply introducing the sample solution into the capillary with vacuum injection for 2 s. The migration times for the Cr(VI) and Cr(III) species were 5.0 and 5.6 min, respectively. The difference in the migration time permits the determination of Cr(III) and Cr(VI) in the presence of each other. Either of the Cr(VI) and Cr(III) species was detected at 256 nm, and the amounts of Cr(VI) and Cr(III) in the sample solution were determined from their calibration curves (Fig. 2.6).

2.3.6 Interferences from foreign ions

The effect of several foreign ions on the determination of Cr(III) and Cr(VI) was investigated; the results are summarized in Table 2.1. For the determination of Cr(III), phosphate and silicate ions caused negative errors by forming the corresponding Keggin-type heteropolyanions with Mo(VI), the formation of which lead to a lack of Mo(VI). Besides the $[CrMo_6O_{24}H_6]^{3-}$ complex, many $[XMo_6O_{24}H_6]^{n-}$ -type heteropoly

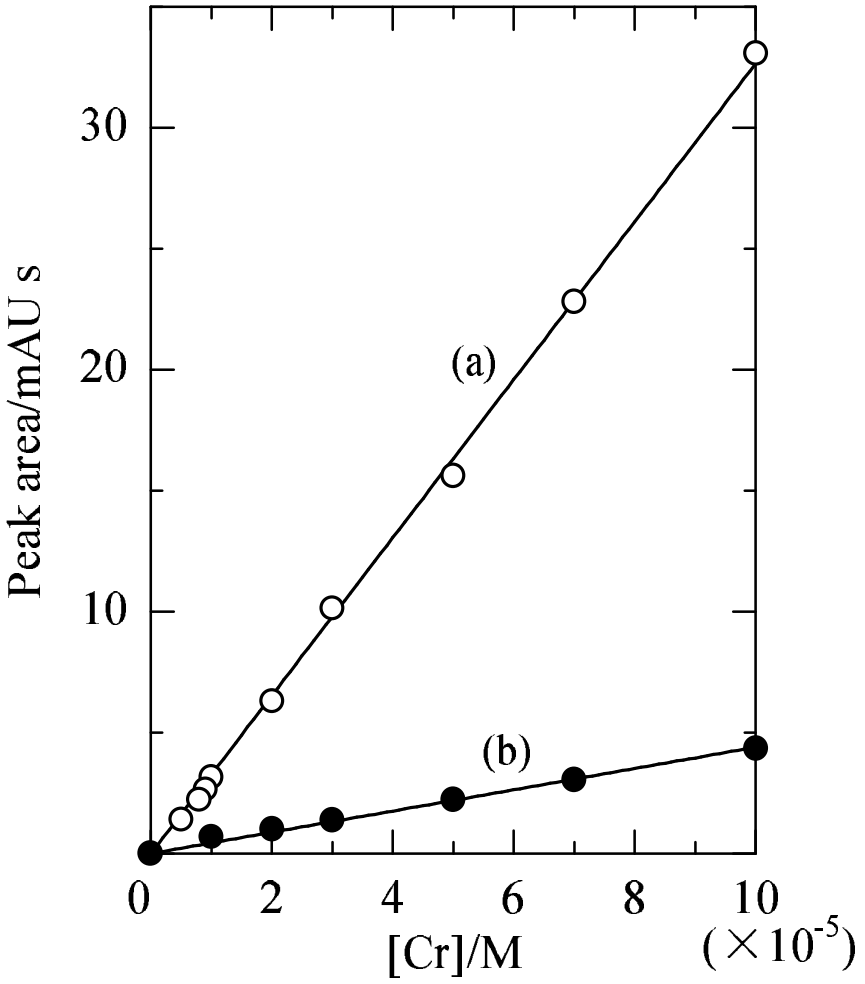

Figure 2.6: Calibration curves for (a) Cr(III) and (b) Cr(VI) in 0.1 M monochloroacetate buffer (pH 2.0) containing 1×10^{-3} M Mo(VI). The migration buffer, 0.1 M monochloroacetate (pH 2.0).

complexes have been isolated, where X=Al(III), Fe(III), Cu(II), Ni(II), Zn(II) and so on, and n=3, 4 [35–38]. There is a possibility that these metal ions can also react with Mo(VI) in a migration buffer of pH 2.0. With the exception of Al(III), however, these metal ions caused only negligible interference, and the details of this reaction will be come back to the chapter 5. In the presence of Al(III), a new peak appeared between the peaks for the Cr(VI) and Cr(III) species. Simultaneously, the peak height due to the Cr(III) species decreased by about 11%. The presence of NaCl at concentrations $< 1\times10^{-2}$ M was tolerable with the determination of Cr(III). As expected, all of the foreign ions studied did not interfere with the determination of Cr(VI).

Table 2.1: Effect of foreign ions on the determination of Cr(III) and Cr(VI).

Ions added as	Concentration/ M	Relative error, % Cr(III)	Cr(VI)
$AlCl_3$	1×10^{-4}	−10.9	2.2
$FeCl_3$	1×10^{-4}	−0.2	−1.9
$Co(NO_3)_2$	5×10^{-4}	−1.3	0.8
$NiCl_2$	1×10^{-4}	−0.4	3.5
$CuSO_4$	5×10^{-4}	−2.8	3.7
$Zn(NO_3)_2$	5×10^{-4}	−3.4	0.2
NaH_2PO_4	1×10^{-4}	−12.3	−0.7
Na_2SiO_3	1×10^{-4}	−9.9	−0.5
NaCl	1×10^{-2}	−1.3	−4.7

Sample: [Cr(III)]=[Cr(VI)]=5×10^{-5} M. 1×10^{-3} M Mo(VI)-0.1 M monochloroacetate buffer (pH 2.0). Migration buffer: 0.1 M monochloroacetate buffer (pH 2.0).

Chapter 3

Simultaneous Determination of Periodate(VII) and Iodate(V)

3.1 Introduction

The determination of iodine species, particularly periodate (I(VII)) is important in organic chemistry, biology and life science, but it is rather difficult to determine I(VII) at the low natural concentration level. Periodate(VII) has been determined so far by spectrophotometric [40–42], polarographic [43,44] and potentiometric [45] methods. Palomares et al. have shown that neutron activation analysis is suitable for the determination of iodine with respect to its high sensitivity [46].

Besides, it is sometimes required to determine the respective concentrations of I(VII) and I(V) in a mixture. According to Honda et al.[47], the direct determination of IO_4^- and IO_3^- is possible by capillary electrophoresis with UV detection at 222 nm. Since both anions have low molar absorption coefficients, the sensitivity of the direct method is accordingly low. There are several ways to im-

prove the sensitivity. Among these is the formation of some complex with a higher molar absorption coefficient. The Na^+ salt of the hexamolybdoperiodate(VII)(5−)($[IMo_6O_{24}]^{5-}$) complex was prepared by heating a reaction mixture of Mo(VI) and I(VII) at very high concentrations [48,49]. However, the existence of the $[IMo_6O_{24}]^{5-}$ anion in solution has not been clarified.

In this chapter, the author has found that the $[IMo_6O_{24}]^{5-}$ anion is formed at low concentrations of Mo(VI) and I(VII), and that the complex-formation reaction is completed very rapidly, even at room temperature. Since the $[IMo_6O_{24}]^{5-}$ anion possesses a much greater molar absorption coefficient than the free IO_4^- ion, the sensitivity for the determination of I(VII) can be improved through complex-formation. On the other hand, no complex-formation reaction of Mo(VI) with I(V) occurred.

In Chapter 2, The author described that a simple and sensitive method for the simultaneous determination of Cr(III) and Cr(VI) by capillary electrophoresis was developed on the basis of the formation of the $[Cr^{III}Mo_6O_{24}H_6]^{3-}$ complex. Similarly, the present study was undertaken to establish a method for the simultaneous determination of I(VII) and I(V), because two peaks corresponding to the migrations of $[IMo_6O_{24}]^{5-}$ and IO_3^- were well-separated in the electropherogram, and the peak heights were linearly dependent on the respective concentrations of I(VII) and I(V). The detection limits of I(VII) and I(V) were 1×10^{-6} and 2×10^{-5} M, respectively.

3.2 Experimental

3.2.1 Apparatus

All apparatus used were described in Chapter 2.

3.2.2 Reagents

All of the reagents were of analytical grade. Standard solutions of I(VII) and I(V) were prepared by dissolving $NaIO_4$ and KIO_3, respectively. The water used was de-ionized and distilled.

3.2.3 Preparation of $(NH_4)_5[IMo_6O_{24}]\cdot 3H_2O$

The following preparative method was established to characterize the hexamolybdoperiodate(VII)(5−) complex in the solid state. The pH of a 100 ml solution containing 6.0 g of $Na_2MoO_4\cdot H_2O$ and 1.2 g of $NaIO_4$ was adjusted to 4.5 with HCl. After the solution was heated at 80°C for 30 min, 10.7 g of NH_4Cl was added, and the resulting colorless solution was allowed to stand in a refrigerator. In a few days, there appeared a white precipitate, which was collected by filtration, washed with water and ethanol, and air-dried. The precipitate was further purified by recrystallization from a 50% (v/v) ethanol-water solution. Anal. Calcd for $(NH_4)_5[IMo_6O_{24}]\cdot 3H_2O$: Mo, 46.8; I, 10.3; NH_4^+, 7.33; H_2O, 4.4%. Found: Mo, 46.7; I, 10.1; NH_4^+, 7.15; H_2O, 4.5%. IR (1000–400 cm^{-1}): 938, 896, 688, 626, 538, 472 cm^{-1} (Fig. 3.1).

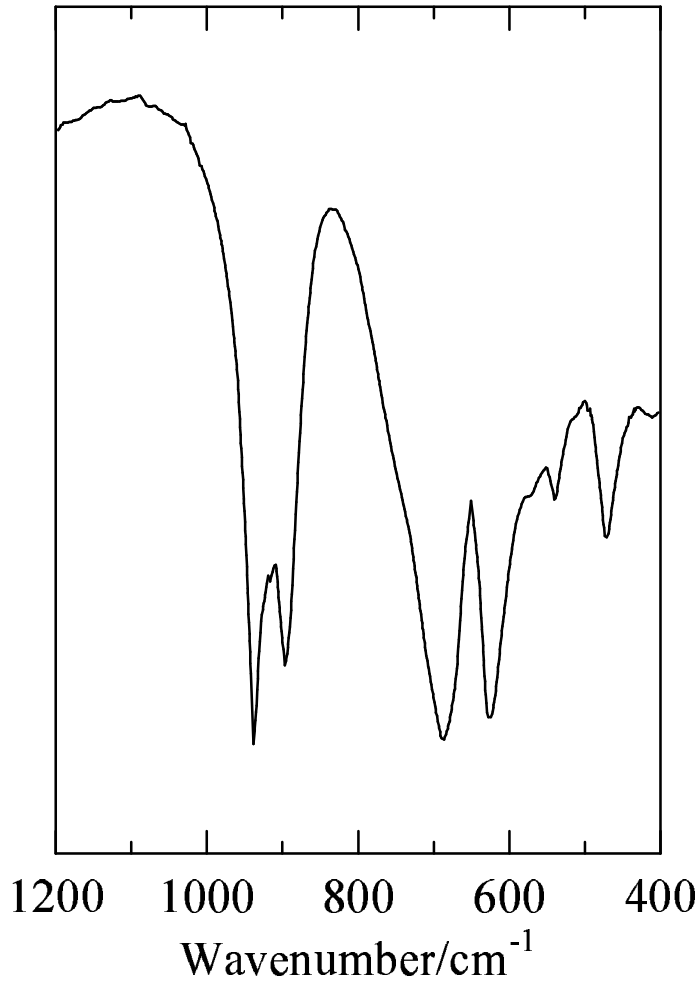

Figure 3.1: An IR spectrum of $(NH_4)_5[IMo_6O_{24}]\cdot 3H_2O$ in a KBr pellet.

3.3 Results and Discussion

3.3.1 Formation of the $[IMo_6O_{24}]^{5-}$ anion in an aqueous solution

The absorption spectra for 1×10^{-4} M I(VII), 6×10^{-4} M Mo(VI) and a mixture of 1×10^{-4} M I(VII) + 6×10^{-4} M Mo(VI) in an aqueous solution of pH 4.5 are shown in Fig. 3.2. The solution containing both I(VII) and Mo(VI) showed a spectrum completely different from a simple additivity of a spectrum for each component (Fig. 3.2(c)), indicating the formation of a heteropoly complex. In order to obtain the optimal pH conditions for the formation of the heteropoly complex, the absorbance values at 280 nm were measured as a function of the pH for a mixture of 2×10^{-5} M I(VII) and 1.2×10^{-4} M Mo(VI). The absorbance values due to the $[IMo_6O_{24}]^{5-}$ complex were calculated on the basis of the molar-extinction coefficients of the $[IMo_6O_{24}]^{5-}$ complex and of Mo(VI) species at the corresponding pH values. The results are shown in Fig. 3.3. The formation of the heteropoly complex became maximal in the pH range of 3–4.5, where the formed heteropoly anion is stable for at least one week, as judged by no change in the absorbance values. On the other hand, no complex formation of I(V) with Mo(VI) occurred.

The compositional ratio of I/Mo in the heteropoly complex was studied by the usual mole-ratio method at 280 nm. In this procedure, the I(VII) concentration was varied in the range of 1×10^{-5}–4×10^{-5} M while keeping the Mo(VI) concentration at 1.2×10^{-4} M. The results demonstrated an I/Mo ratio of 1/6, which indicates the formation of

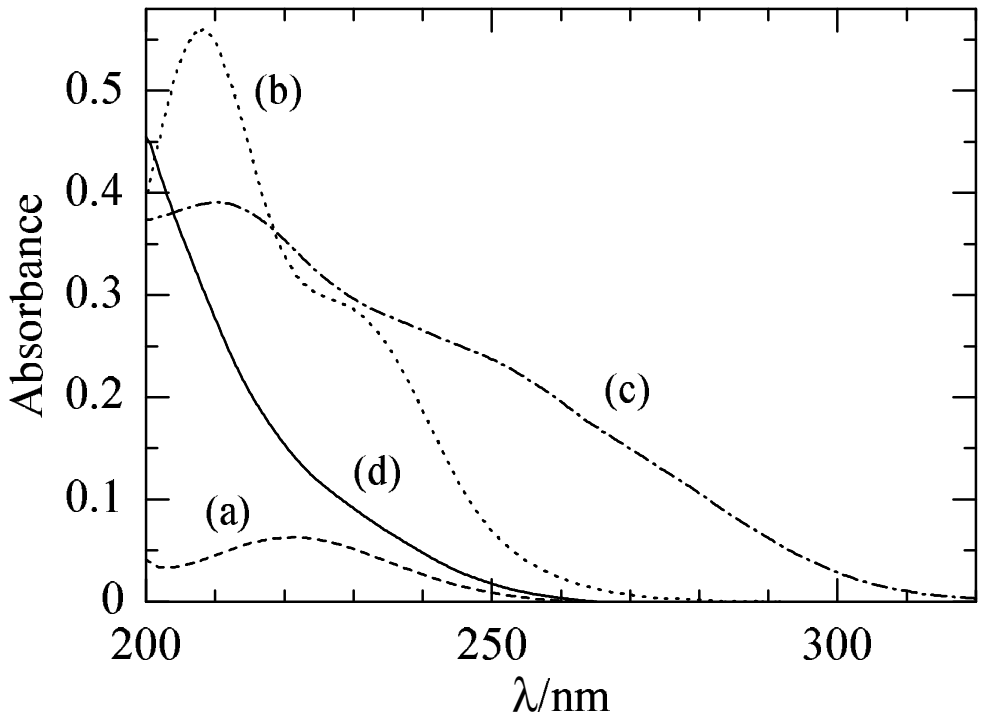

Figure 3.2: Absorption spectra for (a) 1×10^{-4} M I(VII), (b) 6×10^{-4} M Mo(VI), (c) a mixture of 1×10^{-4} M I(VII)+6×10^{-4} M Mo(VI), (d) 1×10^{-3} M I(V) in an aqueous solution (pH 4.5). Path length, 1 mm.

the $[IMo_6O_{24}]^{5-}$ complex, even at such low concentrations of I(VII) and Mo(VI). From a comparison of Fig. 3.2(a) with Fig. 3.2(c), it follows that the molar absorption coefficient for I(VII) is increased by 7–8 times through the formation of the $[IMo_6O_{24}]^{5-}$ complex. Therefore, this complex-formation reaction was applied to the sensitive determination of I(VII) by capillary electrophoresis with UV detection. In addition, it seems possible to determine both I(VII) and I(V) in the

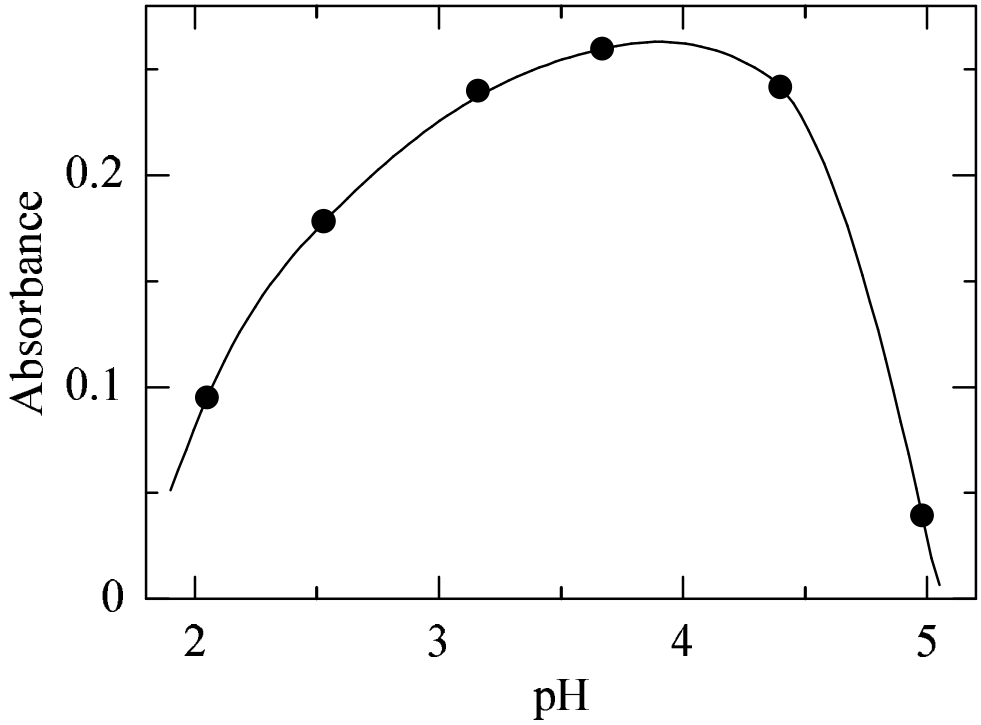

Figure 3.3: Relationship between the pH and the absorbance at 280 nm for an aqueous solution of 2×10^{-5} M I(VII)+1.2×10^{-4} M Mo(VI). Path length, 1 cm.

mixture, because IO_3^- showed an absorption spectrum at wavelengths < 250 nm. In this study, a wavelength of 220 nm was chosen as being optimum for the detection of $[IMo_6O_{24}]^{5-}$ and IO_3^-.

3.3.2 Effect of the Mo(VI) concentration on the electropherogram

The following experiments were carried out to optimize the Mo(VI) concentration in a sample solution to be tested. The test solutions

were prepared by varying the Mo(VI) concentration (1×10^{-3}–5×10^{-2} M) while keeping [I(VII)]=5×10^{-5} M and [I(V)]=5×10^{-4} M in 5×10^{-2} M malonate buffer (pH 4.0). These solutions were introduced into the capillary, and electropherograms were recorded. In a series of electrophoretic measurements, 5×10^{-2} M malonate buffer (pH 4.0) was also used as a migration buffer. As expected, the peak-height for I(V) was independent of the Mo(VI) concentration, since no complex-formation between Mo(VI) and I(V) occurred. The peak due to the $[IMo_6O_{24}]^{5-}$ complex grew with an increase in the Mo(VI) concentration. At Mo(VI) concentrations above 1×10^{-2} M, however, the baseline in the electropherogram was unstable and noisy. Therefore, the Mo(VI) concentration of 1×10^{-2} M was chosen as being optimum.

3.3.3 Choice of the migration buffer and the applied voltage

In order to optimize various conditions for the capillary electrophoretic separation of I(VII) and I(V), the following experiments were carried out with a test solution containing 1×10^{-4} M I(VII), 1×10^{-4} M I(V), 1×10^{-2} M Mo(VI) and 5×10^{-2} M buffer (the same as the migration buffer). At first, tartarate, formate, acetate, monochloroacetate and malonate buffer solutions of pH 2–5 were examined in order to choose a proper migration buffer. Among these buffer solutions, the best results regarding the separation of I(V) and I(VII) and their peak-shapes were obtained with the use of 5×10^{-2} M malonate buffer as the migration buffer.

The effect of the buffer pH on the electropherogram was investi-

gated; the results are shown in Fig. 3.4. As shown in Fig. 3.4(a), two peaks appeared at pH 2.5; peak (i) is due to the $[IMo_6O_{24}]^{5-}$ anion, and peak (iii) is due to IO_3^-. Although no peaks due to the free isopolymolybdate species appeared within 20 min, peak (i) due to the $[IMo_6O_{24}]^{5-}$ anion was not so well-shaped under these conditions. With an increase in the pH, peak (i) increased in height. Simultaneously, the isopolymolybdate species, being changed with the variation in the pH values [39], migrated much faster (Fig. 3.5), and appeared as peak (ii). Since the respective migration times for I(VII) and I(V) were practically unchanged, peak (ii) overlapped with peak (iii) around pH 3.5 (Fig. 3.4(b)), which made it difficult to determine both I(VII) and I(V) simultaneously. With a further increase in the pH, the isopolymolybdate species migrated faster than I(V), and three peaks for I(VII), Mo(VI) and I(V) were well-separated in the pH range of 3.8–4.3 (Fig. 3.5).

Figure 3.6 shows the relationship between the peak heights due to $[IMo_6O_{24}]^{5-}$ and IO_3^- and the pH values for aqueous solutions containing 2×10^{-5} M I(VII), 1.2×10^{-4} M Mo(VI) and 5×10^{-2} M buffer. As shown in Fig. 3.6(a), peak (i) was obtained in the pH range of 2–5. These results are in good agreement with the spectrophotometric observations shown in Fig. 3.3, indicating that peak (i) is actually due to $[IMo_6O_{24}]^{5-}$. It was found that the peak height became highest at around pH 4. On the other hand, the peak height for I(V) was practically unchanged in the pH range of 3–5. From these observations, a buffer pH of 4.0 was chosen as being optimum; the electropherogram showed sharp and reproducible peaks for both I(VII) and I(V) under

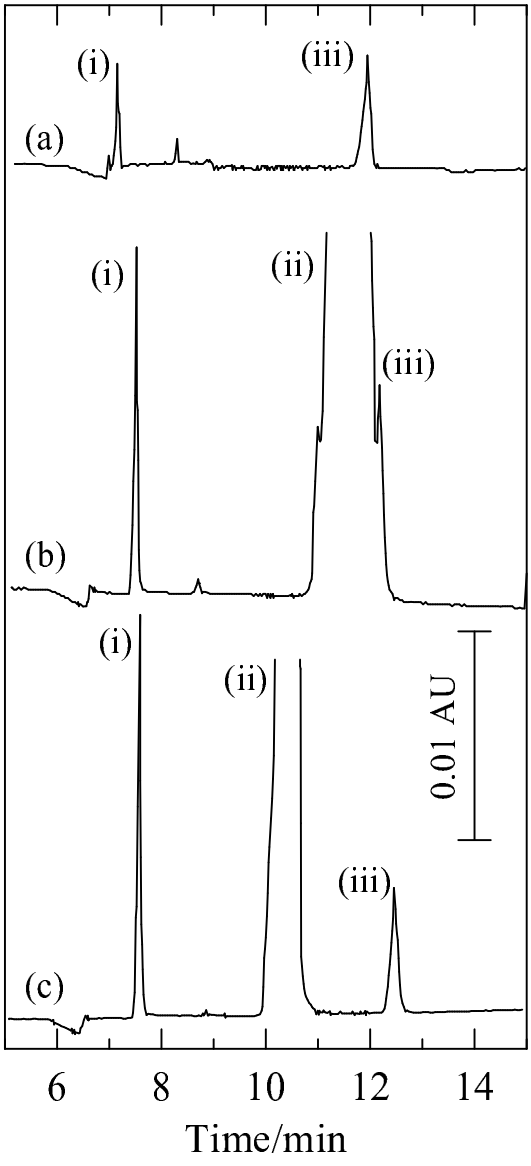

Figure 3.4: Electropherograms for a test solution containing 1×10^{-4} M I(VII), 1×10^{-3} M I(V), 1×10^{-2} M Mo(VI) and 5×10^{-2} M malonate buffer (the buffer pH was adjusted to be the same as the migration buffer). pH values of the migration buffer (5×10^{-2} M malonate buffer): (a) 2.5; (b) 3.5; (c) 4.0. (i) I(VII); (ii) Mo(VI); (iii) I(V).

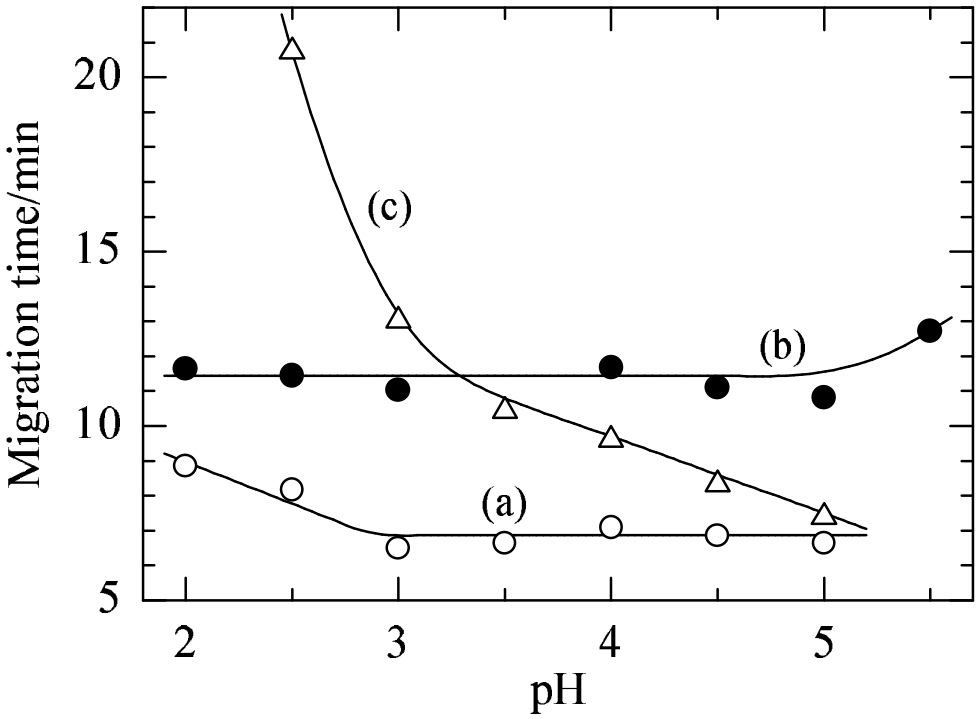

Figure 3.5: Relationship between the pH and the migration times ((a) I(VII); (b) I(V); (c) Mo(VI)) for an aqueous solution of 2×10^{-5} M I(VII), 1×10^{-4} M I(V) and 1.2×10^{-4} M Mo(VI).

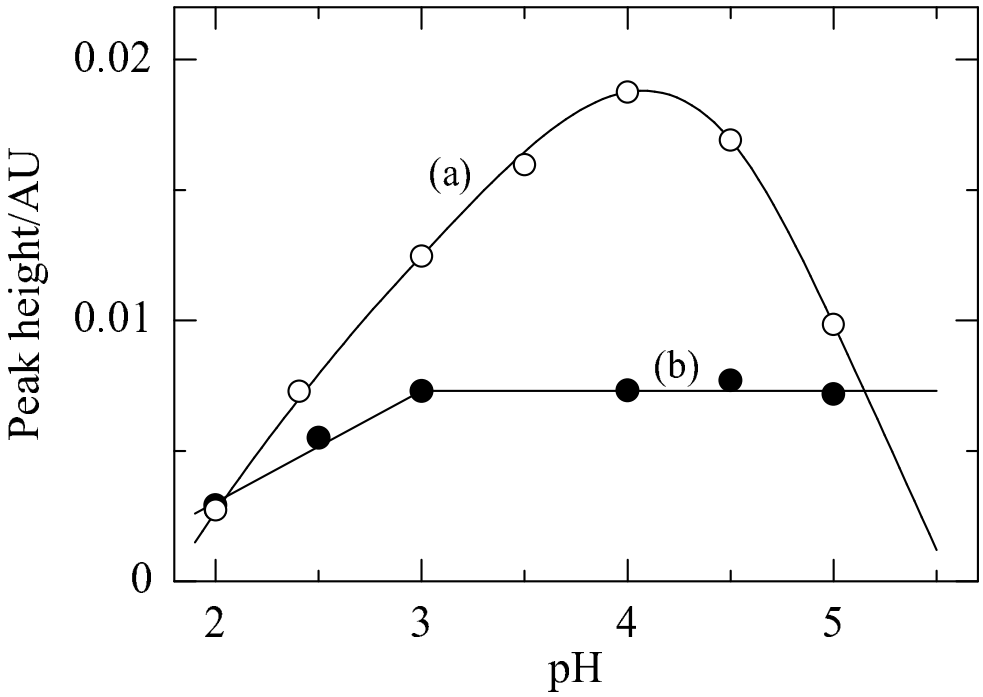

Figure 3.6: Relationship between the pH and the peak-heights ((a) I(VII); (b) I(V)) for an aqueous solution of 2×10^{-5} M I(VII), 1×10^{-4} M I(V) and 1.2×10^{-4} M Mo(VI).

these conditions. Electropherograms were recorded by varying the applied voltage from -5 to -20 kV. The optimum applied voltage was found to be -15 kV.

3.3.4 Recommended procedure for the simultaneous determination of I(VII) and I(V)

The capillary was filled with 5×10^{-2} M malonate buffer (pH 4.0) before sample injection. A 5 ml portion of 0.2 M malonate buffer (pH

4.0) was placed in a 20 ml volumetric flask. After the addition of 2 ml of 0.1 M Mo(VI), an appropriate amount of samples containing of I(VII) and I(V) was added, and the solution was diluted to the mark with distilled water. An electrophoretic analysis was made by introducing the sample solution into the capillary with vacuum injection for 2 s. Migrated I(VII) and I(V) species were detected at 220 nm. The migration times for the I(VII), free isopolymolybdate and I(V) species were 7.7, 9.6 and 11.7 min, respectively. The difference in the migration times was large enough to determine the respective concentrations of I(VII) and I(V) in the mixture. The amounts of I(VII) and I(V) in the sample solution were determined by comparisons with their calibration curves.

On the basis of these findings, calibration curves were obtained by varying the respective concentrations of I(VII) and I(V) while maintaining 1×10^{-2} M Mo(VI) and 5×10^{-2} M malonate buffer (pH 4.0). The peak heights showed a linear dependence on the concentrations of I(VII) and I(V) in the ranges of 2×10^{-6}–2×10^{-4} M and 5×10^{-5}–2×10^{-3} M, respectively. The calibration line curved downward from the linear plot at I(VII) concentrations $> 2\times10^{-4}$ M, owing to the lack of Mo(VI).

3.3.5 Interference from foreign ions

The interference from several foreign ions was studied; the results are shown in Table 3.1. For determining I(VII) and I(V), Cl^-, Br^-, ClO_3^-, ClO_4^- and BrO_3^- had only negligible interference. It is well

Table 3.1: Effect of foreign ions on the determination of I(VII) and I(V).

Ions added as	Concentration/ M	Relative error, % I(VII)	I(V)
NaCl	5×10^{-4}	0.6	−0.6
NaBr	5×10^{-4}	2.1	−2.7
$KClO_3$	5×10^{-4}	3.0	−0.4
$NaClO_4$	5×10^{-4}	−0.6	1.8
$NaBrO_3$	5×10^{-4}	−3.1	−0.5
NaH_2PO_4	1×10^{-4}	−0.7	1.1
Na_2SiO_3	1×10^{-4}	−1.0	0.6

Sample: [I(VII)]=5×10^{-5} M, [I(V)]=5×10^{-4} M, 1×10^{-2} M Mo(VI), 5×10^{-2} M malonate buffer (pH 4.0). Migration buffer; 5×10^{-2} M malonate buffer (pH 4.0). Applied voltage; −15.0 kV.

known that phosphate and silicate can form various types of heteropoly complexes in acidic solutions [50]. However, phosphate did not interfere with the determination of I(VII), probably because no complex-formation occurred under the recommended conditions of pH 4. Although silicate produced a pair of peaks in the electropherogram, due to the formation of a mixture of α- and β-Keggin type heteropoly complexes [51,52], its presence caused no serious errors, because the peaks for the Si(IV), I(VII) and I(V) species were well-separated.

Chapter 4

Stacking Effect on CE Analysis Based on the Formation Heteropolyoxomolybdate

4.1 Introduction

In Chapters 2 and 3, oxidation state analyses of Cr(VI) and Cr(III), and I(VII) and I(V) were made on the basis of the formation of the hexamolybdo-complexes at room temperatures, respectively. However, these sensitivities were slightly inferior to conventional analytical methods such as ion chromatography or spectrophotometry. The lower sensitivity in CE is due to the short path length of UV-visible detector, and the path length can not be change because the capillary tubes used as UV-visible cells. Therefore, a new detection is expected to improve the sensitivity. Recently, the detection method in CE analysis has been developed with mass spectra [53], fluorescence [54,55], conductivity [56,57], electrochemical detection [56,58–64] and

so on. The pre-concentration has been applied to the supersensitivity of CE analysis. The sample stacking with the online pre-concentration methods has been studied by a lot of research workers in recent years. Generally, there are two methods of the sample stacking, which are called the "field-amplified" (FA) stacking and the "transitional isotachophoretic" (ITP) stacking, respectively.

The field-amplified stacking, which utilizes electrokinetic property due to a difference of conductivity between migration buffer and sample solution, was reported by Mikkers et al. in 1979 [65–67]. In these articles, they demonstrated the use of comparatively large-diameter, 200 μm i.d., Teflon capillaries for free solution electrophoresis. There are many investigations using field-amplified stacking in CE up to the present [68–87]. Three different types of field-amplified stacking are known, namely normal stacking (NS), large volume sample stacking (LVSS) and electrokinetic injection (EI), in which the principle of preconcentration is the same in all cases.

Owing to lower conductivity of a sample solution compared with a migration buffer, the analyte ions move faster in sample zone than in the migration buffer. Then, the analyte ions are collected at the boundary between the front of sample zone and the migration buffer, which brings about high plate numbers for the analyte peaks in the electropherogram (Fig. 4.1(a)). On the contrary, when the conductivity of the sample buffer is higher than the migration buffer, zone broadening takes place, and gives flat peaks (Fig. 4.1(b)) [74].

Normal stacking is the simplest among sample stacking modes. It is done by dissolving the sample in a low conductivity matrix and

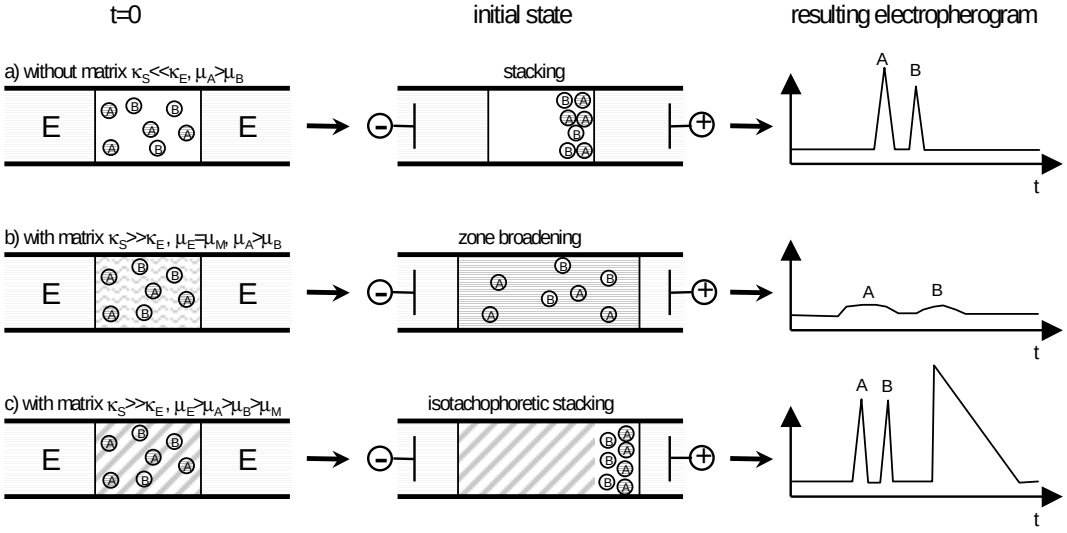

Figure 4.1: Influence of the sample contents on the stacking process the stacking process and the resulting electropherograms.

by injecting the resulting sample solution hydrodynamically or hydrostatically. As stated earlier, focusing happens at the interface between the low conductivity matrix and the BGE, due to the abrupt change in electrophoretic velocity. There are several means by which the conductivity of sample zone is decreased. Simply, the sample solution is diluted, or the weak buffer is added to the sample solution. Specially, NS stacking using acetonitrile (CH_3CN) as BGE; the so-called acetonitorile stacking (AS), which is applied to the biochemical analysis. A limitation in NS is the short optimum sample plug length that can be injected into the capillary without loss of separation efficiency or resolution. Concentration factors of around 10 are usually obtained with NS, improving concentration limit of detection (LOD) a whole order of magnitude.

When the volume of sample introduced is greater than that found optimum in NS, the sample matrix must be pumped out from the capillary in order to preserve separation efficiency. This stacking method is termed as large volume sample stacking (LVSS). Pumping may be performed with external pressure or with electroosmotic flow (EOF), which stream from anode to cathode. The direction of pumping is always opposite that of the electrophoretic movement of charged analytes. The velocity of pumping should also be lower than the electrophoretic velocity of the charged analytes.

Sample stacking with electrokinetic injection is first described by Chien and Bugi [73]. The sample is prepared in a low conductivity matrix and the resulting sample solution is injected using voltage. Usually positive or negative ions can be concentrated effectively using a single electrokinetic injection. Sample stacking with electrokinetic injection provided larger sensitivity enhancements compared with hydrodynamic injection [88].

On the other hand, J. Boden and K. Bächmann described the transitional isotachophoretic stacking in 1996 [89]. Thereafter, there are many investigations on ITP stacking [90–93]. It is assumed that a sample solution is a homogeneous mixture of the analyte and the additive ions, which have a lower mobility than migration buffer. On applying an electric field, the additive and analyte ions migrate from the sample zone to the boundary of the sample zone and the migration buffer zone with peculiar velocity, and so the transitional isotachophoretic state occurs in the typical profile of conductivity and concentration being regulated according to the Kohlraush-regulating-

function [66,89]. Therefore, the analyte ions is pre-concentrated at the front of the boundary between additive ions and migration buffer (Fig. 4.1(c)). In contrast, for a high mobile additive ions and a low mobile migration buffer, this online pre-concentration takes place at the rear side of the additive ions.

In this chapter, the author described the sample stacking effect to improve separation efficiency and detection limit of CE analysis based on the formation of heteropolyoxometalates. According to the field-amplified stacking or the transitional isotachophoretic stacking, the migration peaks due to the Anderson-type complex of $[CrMo_6O_{24}H_6]^{3-}$ and $Cr_2O_7{}^{2-}$ became sensitive and well separated. Similarly, isomers of a Keggin-type dodecamolybdosilicate with approximately the same migration time could be separated satisfactorily. Furthermore, the transitional isotachophoretic stacking was effective on the determination of phosphate based on the formation of a Keggin-type complex in aqueous-CH_3CN media.

4.2 Experimental

4.2.1 Apparatus

Analyses were performed on a CAPI–3200Q capillary electrophoresis system (Otsuka Denshi, Osaka, Japan), equipped with a photo diode array UV-visible detector and a data collecting system. The used fused-silica capillaries (GL Sciences, Tokyo, Japan) were 62.2 cm in total length, 50 cm in effective length from the sample injection port

to the detector, and had an I.D. of 75 μm.

Other apparatus used were described in Chapter 2.

4.2.2 Reagents

Methanesulfonic acid, trifluoromethanesulfonic acid and *p*-xylene-2-sulfonic acid (XSA) were purchased from Tokyo Kasei (Tokyo, Japan). The water used was deionized and purified with a MILLI–Q Labo system (Millipore, Tokyo, Japan). Other reagents used were described in Chapter 2.

4.3 Results and Discussion

4.3.1 Stacking effect on CE analysis of $[CrMo_6O_{24}H_6]^{3-}$

In the first place, the author investigated an influence of dissimilar buffer concentration in the sample solutions from migration buffer on the electropherogram. Figure 4.2(a) shows the relationship between concentration of monochloroacetate buffer in sample solution and the peak heights or migration times on CE analysis of $[CrMo_6O_{24}H_6]^{3-}$. The 100 mM monochloroacetate solution of pH 2.5 was used as migration buffer. On increasing the buffer concentration in sample solution, the peak heights of hexamolybdochromate became low because of zone broadening (Fig. 4.1(b)). On the other hand, as the amount of monochloroacetate was decreased, the ionic strength of sample zone decreased. Because of the field-amplified stacking, the $[CrMo_6O_{24}H_6]^{3-}$ complexes collected at the boundary of the front of sample zone and

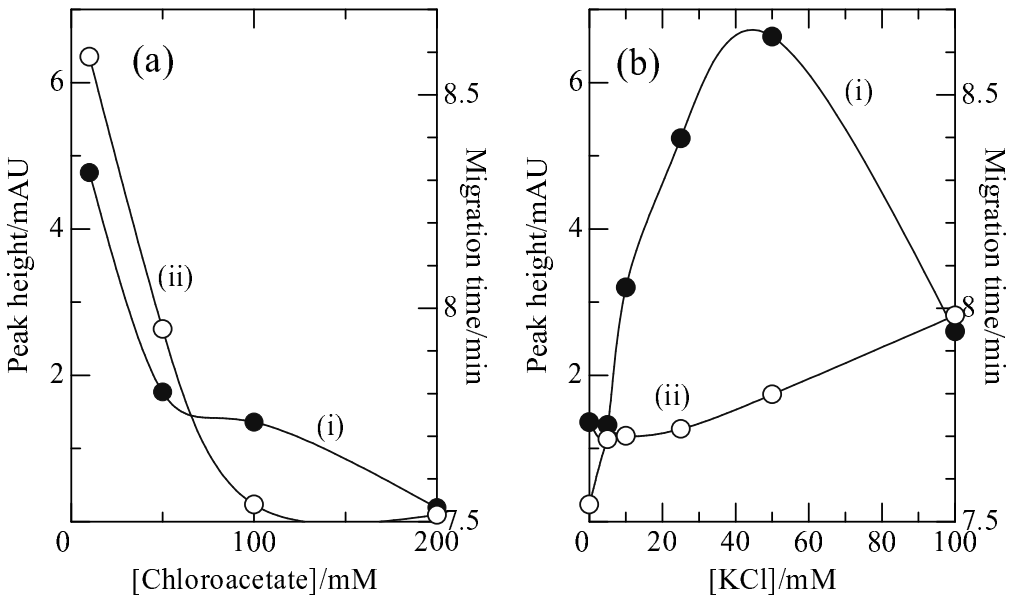

Figure 4.2: (i) Peak heights or (ii) migration times for $[CrMo_6O_{24}H_6]^{3-}$ complexes as a function of concentration of (a) monochloroacetate buffer and (b) KCl for a 1 mM Mo(VI)–1×10^{-5} M Cr(III) system containing an amount of monochloroacetate buffer (pH 2.5) and KCl. Migration buffer; 0.1 M monochloroacetate buffer (pH 2.5). Detection; 254 nm. Applied voltage; −12.0 kV. Injection time; 30 s.

the migration buffer, and the peak profiles of this complex became sharp on the electropherogram (Fig. 4.1(a)). This species migrated much slower, and the peak height in the presence of 10 mM monochloroacetate became three times as higher as that in the presence of 100 mM monochloroacetate.

In order to study the transitional isotachophoretic stacking, an appropriate amount of a KCl solution was added to a sample solution and

the electropherogram was recorded. Figure 4.2(b) shows that the relationship between the concentration of KCl in a sample solution and the peak heights or migration times on CE analysis of $[CrMo_6O_{24}H_6]^{3-}$. As the amount of KCl was increased, the transitional isotachophoretic state due to Cl^- as leading ion was increased in time (Fig. 4.1(a)). At KCl concentration equal 50 mM, the peak height of $[CrMo_6O_{24}H_6]^{3-}$ is five times as higher as that in the absence of KCl in a sample solution. However, at KCl concentration $>$ 50 mM, the peak height and area of Cr-complex decreased. This behavior is probably due to the decrease of an amount of produced $[CrMo_6O_{24}H_6]^{3-}$ complex. This complex migrated much slower as increasing KCl concentrations in sample solutions.

Electropherograms were recorded with the variation of injection times as shown Fig. 4.3. CE analyses without both stacking effects seemed simply to extend sample zone length, and the peak profiles were rectangles (Fig. 4.3(a)). On the other hand, both stacking effects were effective in supersensitive analysis even at 150 s. At injection times $>$ 150 s, however, the peak profiles destroyed, and became near rectangles with the field-amplified stacking. With the transitional isotachophoretic stacking, the peaks due to Cr(VI) and Cr(III)-complex overlapped owing to the exceeding stacking states.

On the basis of these findings, the optimum determination ranges and detection limits of Cr(IV) and Cr(III) were studied, again. These values are 5–10 time as more sensitive as in Chapter 2 (Table 4.1). It was found that both stacking effects were valid on CE analysis with high sensitivity based on the formation of heteropolyoxomolybdates.

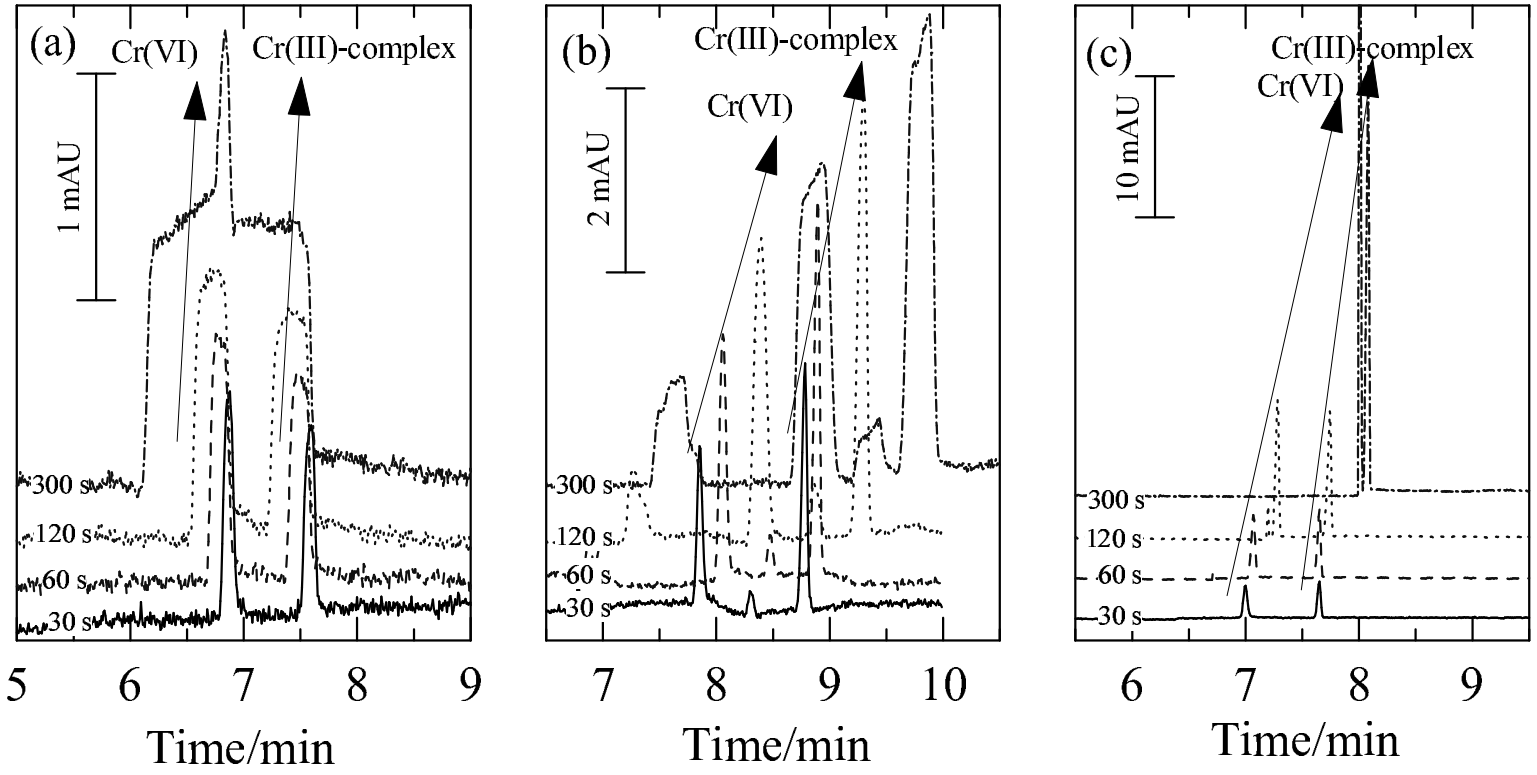

Figure 4.3: Electropherograms for 1 mM Mo(VI)–1×10^{-5} M Cr(III)–1×10^{-4} M Cr(VI)–(a), (c) 0.1 M, (b) 0.01 M monochloroacetate buffer (pH 2.5) systems, (c) containing 0.05 M KCl. Migration buffer; 0.1 M monochloroacetate buffer (pH 2.5). Detection; 254 nm. Applied voltage; −12.0 kV.

Table 4.1: A comparison of the results obtained with and without ITP stacking

Methods	Determination range/M	Detection limit/M
with ITP stacking	5×10^{-7}–1×10^{-4}	2×10^{-7}
without ITP stacking	5×10^{-6}–1×10^{-4}	2×10^{-6}

Cr(III) in 0.1 M monochloroacetate buffer (pH 2.5) and 1 mM Mo(VI) with or without 50 mM KCl. Migration buffer; 0.1 M monochloroacetate buffer (pH 2.5). Applied voltage; −12.0 kV.

4.3.2 Stacking effect on speciation of α- and β-$[SiMo_{12}O_{40}]^{4-}$

It is well-known that a mixture of α- and β-Keggin-type heteropoly complexes are formed from a mixture of Mo(VI) and Si(IV) in acidic solution [51,52]. The chemical equilibrium of these isomers, was investigated by electrochemical and spectrophotometlical methods, the detail of these phenomena has not been made clear because of existence of many other polyoxo-complexes. Therefore, the separation of one from another polyoxo-complexes has been undertaken by mean of chromatographic techniques.

Figure 4.4(a) shows an electropherogram for a 10 mM Mo(VI)–0.05 mM Si(IV)–100 mM monochloroacetate buffer (pH 2.5) system. Without stacking effects, α- and β-Keggin-type heteropoly isomers were recorded as a overlapping peak on the electropherogram, owing to approximately the same electrophoretic mobility. Similar to CE analysis of Cr-complex, the sample solution in which buffer concentration or an amount of chloride such as KCl was reduced provided well defined

peaks due to the respective dodecamolybdosilicate isomers on the electropherograms (Fig. 4.4(b) and (c)). On the basis of these findings, the author investigated the formation and the transformation of α- and β-$[SiMo_{12}O_{40}]^{4-}$ by means of CE method with a filed-amplified stacking effect. As shown in Fig. 4.5, these CE methods enable us to observe the formation and transformation reactions of the dodecamolybdosilicate isomers, being troublesome by electrochemical and spectrophotometlical method.

4.3.3 Stacking effect on CE analysis of $[PMo_{12}O_{40}]^{3-}$

The author described details of determination of phosphate by CE analysis in Chapter 6. Here, it was only demonstrated that the stacking effect on the determination of phosphate. Figure 4.6 shows the electropherograms of a 5×10^{-6} M phosphate–2.5×10^{-3} M Mo(VI)–60% (v/v) CH_3CN system containing each strong acid (50 mM). The peak height of dodecamolybdophosphate increased in the order of HCl, CF_3SO_3H, H_2SO_4, $HClO_4$, CH_3SO_3H and XSA. The peak height in the presence of XSA was approximately 3.5-fold greater than that when HCl was used. These behaviors are due presumably to the state of transitional isotachophoresis, owing to occurred by the addition a large amount of anion to sample solutions [89]. It is common knowledge that the transitional isotachophoretic stacking effect is affected by a difference mobility between sample zone and migration buffer component, and the degree of stacking effect is dependent on the interval of transitional isotachophoretic state of analyte ion.

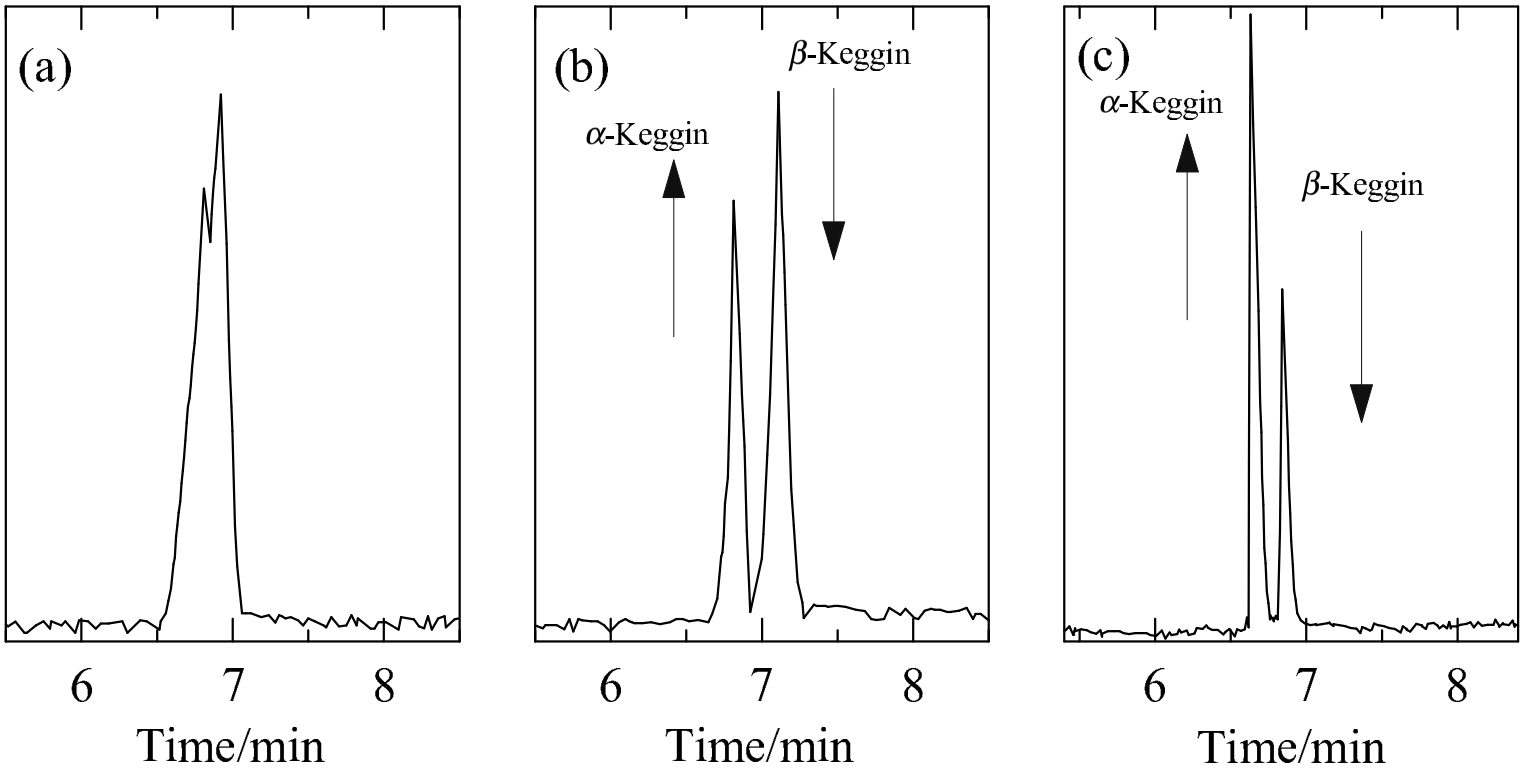

Figure 4.4: Electropherograms for 10 mM Mo(VI)–0.05 mM Si(IV)–(a), (c) 0.05 M, (b) 0.01 M monochloroacetate buffer (pH 2.5) systems (c) containing 0.05 M NH_4Cl. Migration buffer; 0.05 M monochloroacetate buffer (pH 2.5) . Detection; 220 nm. Injection time; 30 s. Applied voltage; −15.0 kV.

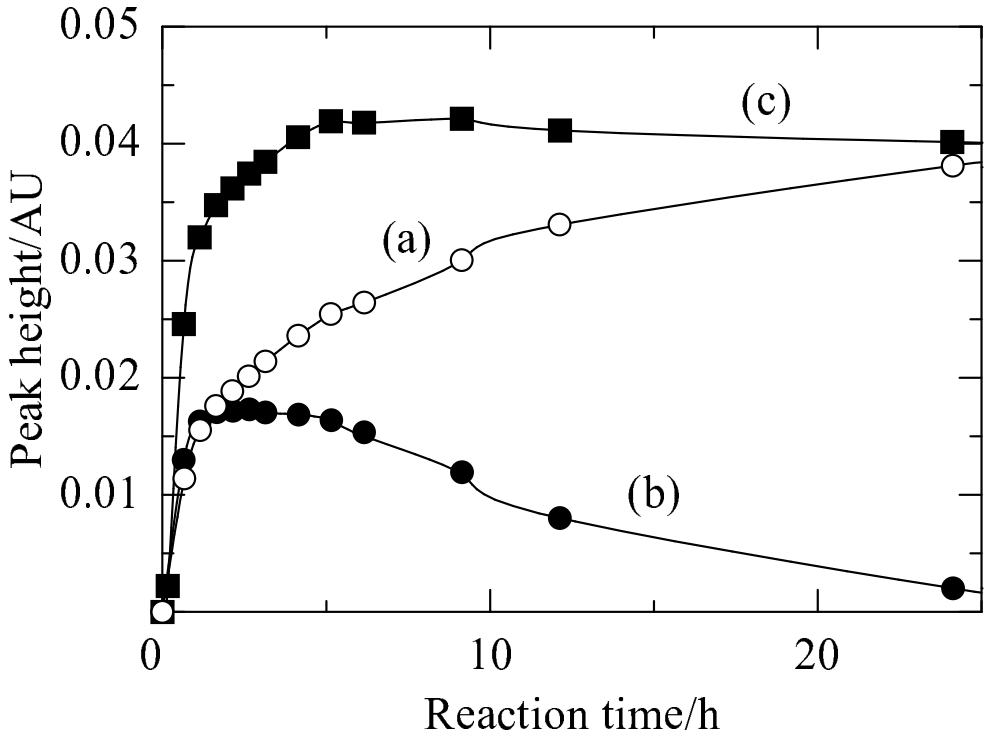

Figure 4.5: Peak heights for α- and β-$[SiMo_{12}O_{40}]^{4-}$ complexes as a function of reaction time for a 1.2 mM Mo(VI)–0.1 mM Si(IV)–0.01 M monochloroacetate buffer (pH 2.5) system. Migration buffer; 0.05 M monochloroacetate buffer (pH 2.5). Detection; 220 nm. Injection time; 30 s. Applied voltage; −15.0 kV.

The author measured an electrophoretic mobility of each anion to prove this stacking behavior (Table 4.2). For the HCl system, the analyte zone broadening takes place, because sample conductivity is higher than a conductivity of the migration buffer and a mobility of sample matrix equals that of the migration buffer. Therefore, a broad peak shape with low peak height and plate numbers appeared on the electropherograms. In the case of a high mobility acid such as H_2SO_4, $HClO_4$ and CH_3SO_3H, an transitional isotachophoretic stacking effect at front of the zone of isopolymolybdates leads to a sharp boundary between the zone of chloride in the migration buffer and the zone of isopolymolybdates. However, a high mobility acid causes the so-called the electromigration dispersion [66,94]. The electromigration dispersion is related to the difference of analyte from matrix on the mobility. Then, the peak height of dodecamolybdophosphate was decreased with an increase in the degree of acid mobility. The $CF_3SO_3^-$ anion specially has approximately the same electrophoretic mobility of dodecamolybdophosphate, both anions may form a mix zone, and migrate together. In this case, broad peak shape of dodecamolybdophosphate consequently appeared on the electropherograms. As with the high mobility acid, the transitional isotachophoretic state occurs between the zone of dodecamolybdophosphate and matrix anions in the case of a low mobility acid such as benzenesulfonic acid (BSA), *p*-toluenesulfonic acid (TSA) and XSA. The well-defined peak shape was therefore obtained and the electromigration dispersion was suppressed in these systems.

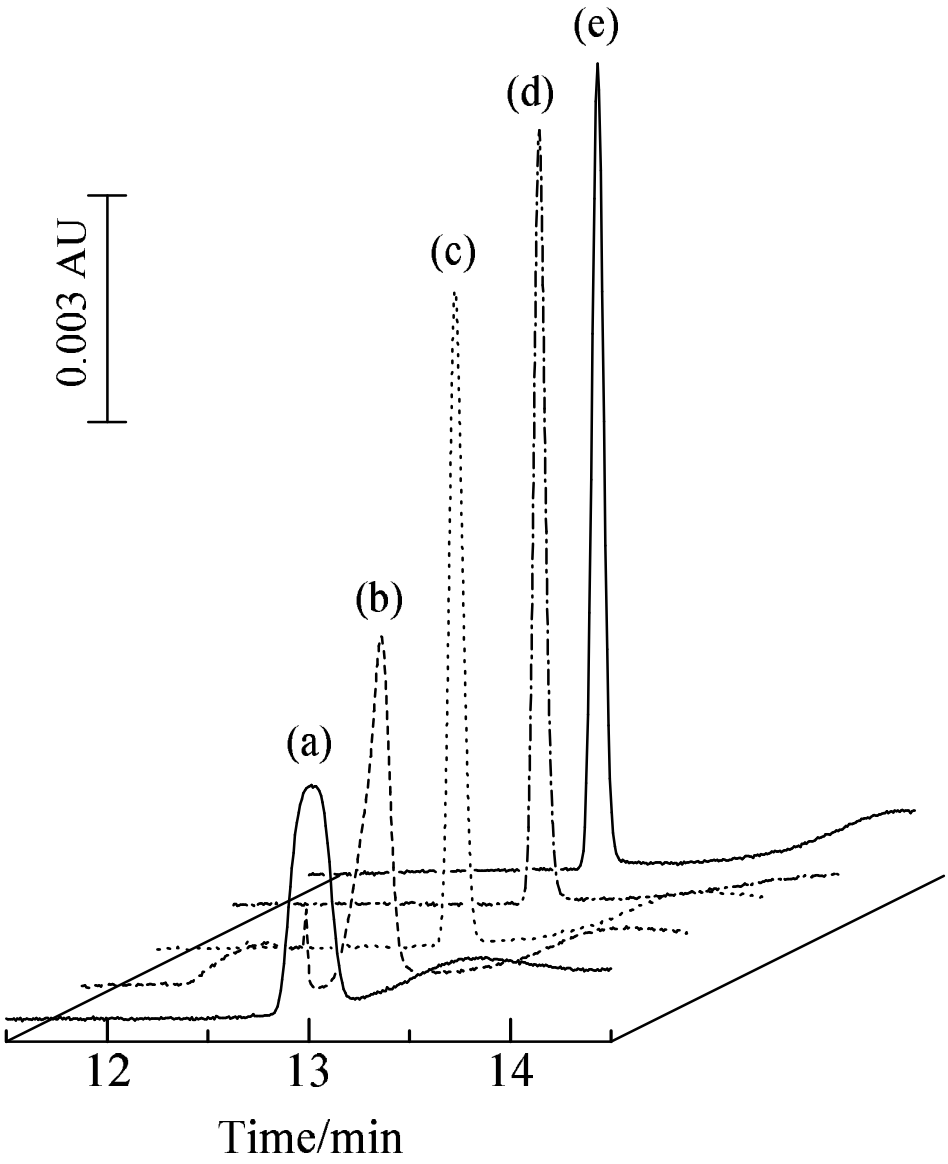

Figure 4.6: Electropherograms for a 5×10^{-6} M Mo(VI)–5×10^{-6} M P(V)–60% (v/v) CH_3CN system containing 0.050 M of (a) HCl, (b) CF_3SO_3H, (c) H_2SO_4, (d) CH_3SO_3H or (e) XSA. The migration electrolyte; 0.050 M HCl–60% (v/v) CH_3CN. Applied voltage; −8.5 kV.

Table 4.2: Effect of electrophoretic mobility on the ITP stacking

Strong acids	$\mu_{ep}{}^{a}$ [$cm^2/V{\cdot}s]{\cdot}10^{-4}$	Peak area[b] [mAU·s]
HCl	6.1	2.84
H_2SO_4	5.8	8.62
$HClO_4$	5.5	9.30
CH_3SO_3H	5.4	10.19
CF_3SO_3H	4.5	4.26
BSA	3.7	10.01
TSA	3.6	10.51
XSA	3.4	10.65
$[PMo_{12}O_{40}]^{3-}$	4.5	—
Isopolymolybdates	3.7	—

[a]The electrophoretic mobility were calculated from the measurements with the migration buffer of 0.5 mM Cr(VI)–50 mM HCl–60% (v/v) CH_3CN.

[b]Test solution was a 5×10^{-6} M phosphate–2.5 mM Mo(VI) –60% (v/v) CH_3CN system containing 50 mM each strong acids. The migration buffer; 50 mM HCl–60% (v/v) CH_3CN. Applied voltage; −8.5 kV.

Chapter 5

Simultaneous determination of Al(III) and Ga(III)

5.1 Introduction

In this Chapter, the author described the simultaneous determination of Al(III) and Ga(III) by capillary electrophoresis, which is based on the formation of hexamolybdoalumate(III) and hexamolybdogallate(III) complexes in aqueous-organic solutions.

In general, metal ion analyses by CE methods have been utilized indirect photometric detection with suitable absorbing cations such as imidazole. The determination of metal ions also need complex-forming reagents [95,96], such as hydroxyisobutyric acid [97–99], 18-crown-6 [100], 8-hydroxyquinoline-5-sulphonic acid [97,101] and ethylendiaminetetraacetic acid [12,97,102], because most metal ions have similar mobilities due to their similar size and identical charge. Al(III) and Ga(III) exhibit exceedingly similar chemical behavior [103–107], because few methods have been developed for the simultaneous CE

determination of Al(III) and Ga(III).

It is well known that Al(III) and Ga(III) react with very high concentrations of Mo(VI) at high temperature, resulting heteropolyoxomolybdate complexes are formed. As stated above, the author has found that several heteropolyoxomolybdate complexes are formed at very low concentrations and even room temperatures, and hexamolybdogallate(III)(−3) ($[Ga^{III}Mo_6O_{24}H_6]^{3-}$) is produced under the similar conditions as Cr(III). On the other hand, the formation reaction of hexamolybdoalumate(III)(−3) ($[Al^{III}Mo_6O_{24}H_6]^{3-}$) at very low concentrations, although, undergoes only by heating in aqueous solutions, this reaction completes in an aqueous-organic solvent as the reaction medium without heating. Ga(III) reacts soon with Mo(VI) in aqueous-organic solutions as well as Al(III) does. On the basis of these findings, the author has investigated electrophoretic behavior of these hetero poly anions, and then the peaks on electropherograms due to both Anderson-type complexes become well separated, so that the simultaneous determination of Ga(III) and Al(III) is possible.

The molar absorption coefficient of these polyoxo anions approximately is 10 times larger than of indirect photometric reagents such as imidazole. Owing to highly molar absorptivities, the purpose of this work is the detailed evaluation of hexamolybdoalumate(III) and hexamolybdogallate(III) complexes for the simultaneous and sensitive determination of Al(III) and Ga(III). Attention was paid to the effect of carrier electrolyte parameters on the migration behavior of hexamolybdoalumate(III) and hexamolybdogallate(III) complexes. The feasibility of the method was demonstrated, and was compared with

indirect photometric method.

5.2 Experimental

5.2.1 Apparatus

All apparatus used were described in Chapter 4.

5.2.2 Reagents

All of the reagents were of analytical grade without further purification. Standard solutions were prepared by dissolving $Al(NO_3)_3$ and $Ga(NO_3)_3$, respectively. Triammonium hexamolybdoalumate(III) [38] and triammonium hexamolybdogallate(III) [37], were synthesized from existing procedure.

5.2.3 The Conditions for the indirect photometric determination of Al(III) and Ga(III)

The indirect photometric determination of Al(III) and Ga(III) was carried out from following a precedent investigation [108]. The migration buffer was prepared with a background electrolyte containing 5 mM of imidazole. The pH of migration buffer was adjusted with a bit of 0.5 M sulfuric acid. Sample solutions were prepared by diluting standard solution with purified water. The electrophoretic analysis was made by introducing the sample solution into the capillary with hydrostatic injection for 30 s, or more sensitive determination was made by electrostatic injection [85] for 10 s and applied voltage was

10 kV. A voltage of 22 kV was applied and capillary cartridge temperature was held at 25°C for the separations. Indirect UV detection was employed 214 nm, and electropherograms were recorded.

5.3 Results and Discussion

5.3.1 Formation of the hexamolybdoalumate(III) and hexamolybdogallate(III)

It is well known that Al(III) and Ga(III) react with very high concentrations of Mo(VI) at high temperature as well as Cr(III). The author measured UV-visible spectra of Mo(VI)–Al(III) and Mo(VI)–Ga(III) system, in order to study complex formation reactions of hexamolybdoalumate(III) and hexamolybdogallate(III) in diluted solution.

Figure 5.1 shows the absorption spectra in an aqueous solution of pH 2.5 for 3×10^{-4} M Mo(VI), a mixture of a 3×10^{-4} M Mo(VI) + 5×10^{-5} M Al(III) and of a 3×10^{-4} M Mo(VI) + 5×10^{-5} M Ga(III). The solution of Al(III) and Ga(III) had no absorbance at range 200–400 nm, respectively. The UV-visible spectra of solutions containing Al(III) or Ga(III), and Mo(VI) completely different from a simple additivity of a spectrum for each components (Fig. 5.1(b) or (c)), indicating the formation of a heteropoly complexes even at such low concentrations.

Then, the electropherograms of the hexamolybdoalumate(III) and hexamolybdogallate(III) were obtained under same condition being

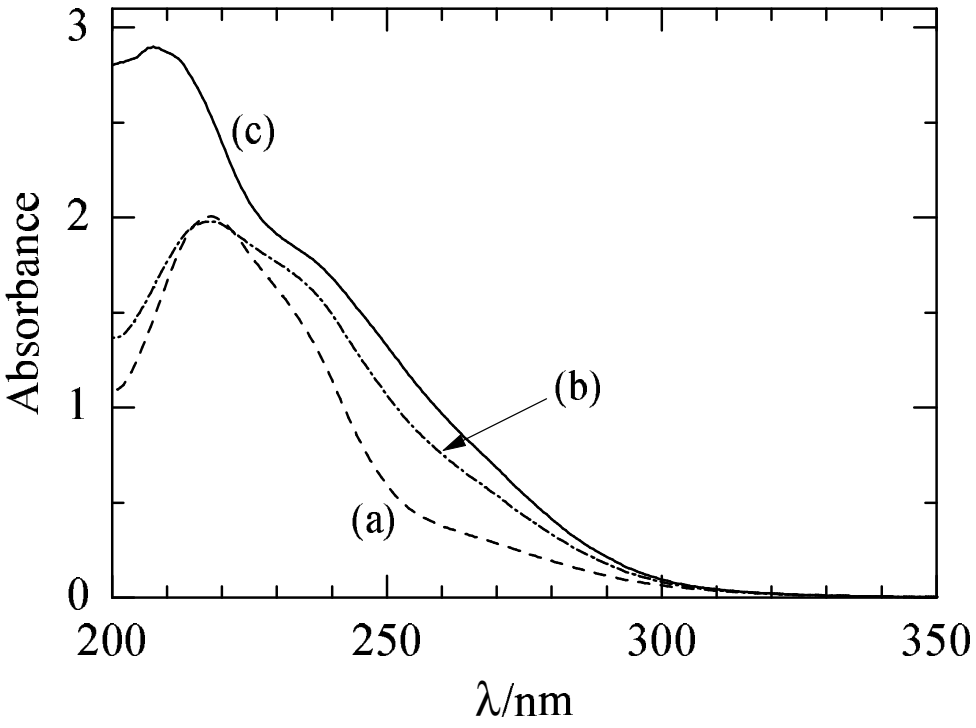

Figure 5.1: Absorption spectra for (a) 3×10^{-4} M Mo(VI), and (b) a mixture of 5×10^{-5} M Al(III)$+3\times10^{-4}$ M Mo(VI) and (c) 5×10^{-5} M Ga(III) $+ 3\times10^{-4}$ M Mo(VI) in an aqueous solution (pH 2.5).

described in chapter 2, so that the peak of $[GaMo_6O_{24}H_6]^{3-}$ was well defined sharp profile. However, the peak height of $[AlMo_6O_{24}H_6]^{3-}$ complex was very lower than Ga(III) complex at room temperature. With heat, the peak due to hexamolybdoalumate(III) grew up, but the determination of Al(III) was not possible because of the peak due to one of the isopolyoxomolybdates, which turned up at the same migration time of $[AlMo_6O_{24}H_6]^{3-}$ anion (Figure 5.2(a)).

Recently, remarkable progress in the preparation of polyoxometalate complexes has been made using water-miscible organic solvents like CH_3CN [109–116]. For the purpose of studying the effect of aqueous-organic solvents on the formation reaction of the isopolyoxomolybdates and $[AlMo_6O_{24}H_6]^{3-}$, an appropriate amount of CH_3CN was added to the test solution, and so the CE measurements were occurred. From these results, it has been found that an amount of formation isopolyoxomolybdate decreased with increasing concentration of CH_3CN in a test solution (Fig. 5.2(b) and Fig. 5.3(c)). In contrast, an adding CH_3CN scarcely effected on an amount of formed Al(III) and Ga(III) complexes (Fig. 5.3(a) and (b)). On the basis of these findings, the optimum concentration of CH_3CN in a test solution is 60% (v/v).

The peak heights for Al(III) and Ga(III) complexes were measured as a function of the reaction time at room temperature, and are shown in Fig. 5.4. The peak heights of Ga(III) had been made experimented in present study were independent of the period, which is denoted as the reaction time. In the presence of 60% (v/v) CH_3CN, the peak area of Al(III) complex grew with the reaction time attained a constant value at a reaction time of 20 min. The sample solution was standing for 20 min at ambient temperature, because reproducible results were obtained even when the Al(III) and Ga(III) complexes were determinated.

The following experiments were carried out to optimize the Mo(VI) concentration in a sample solution to be tested. The test solutions were prepared by varying the Mo(VI) concentration (1×10^{-3}–5×10^{-2}

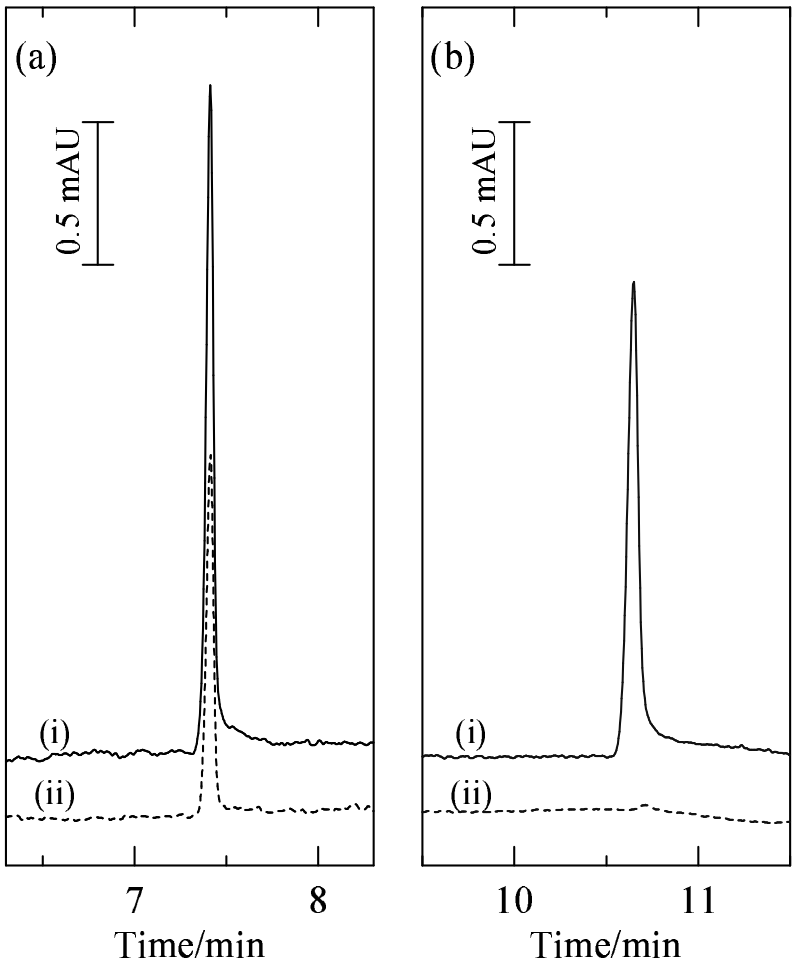

Figure 5.2: Electropherograms for 1×10^{-2} M Mo(VI)–5×10^{-2} M monochloroacetate buffer (pH 2.0) (a) without and (b) with 40% (v/v) CH_3CN systems containing Al(III) (i) 1×10^{-5} M, (ii) none. Measured after (a) heating at 70°C for 20 min and (b) standing at room temperature for 20 min. Migration buffer; 0.1M monochloroacetate buffer (pH 2.0). Applied voltage; −13.0 kV.

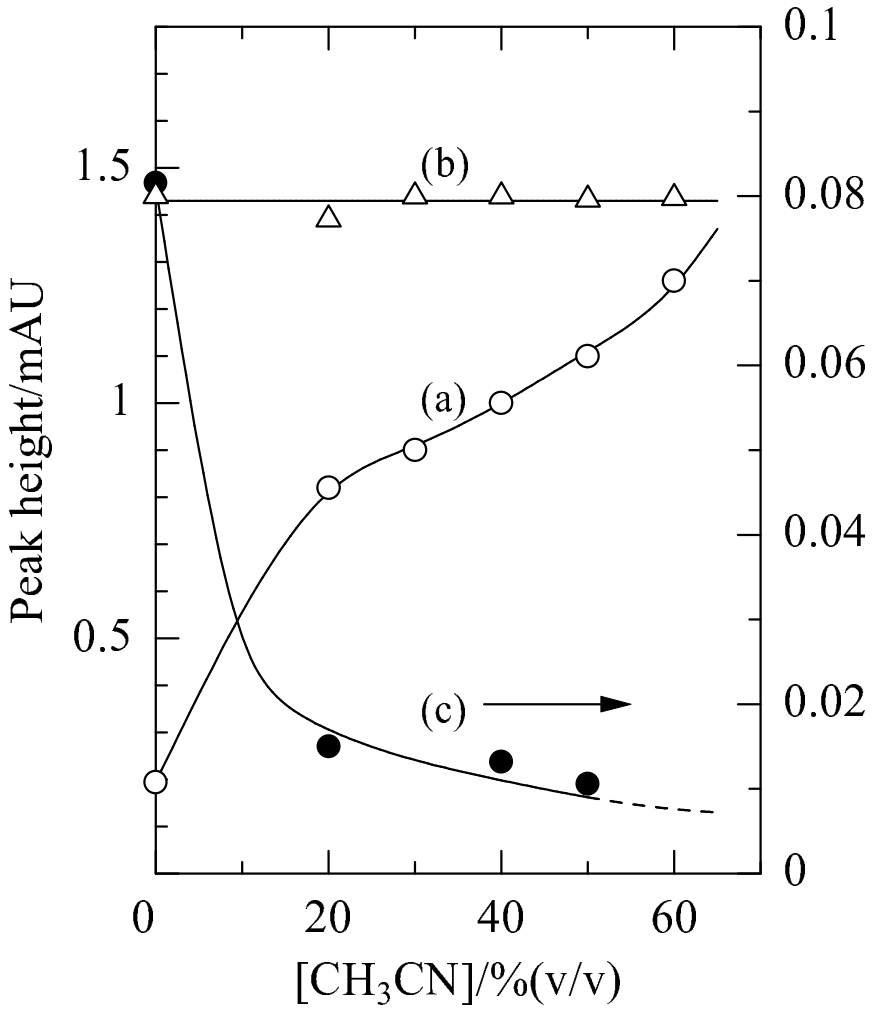

Figure 5.3: Peak height as a function of the CH_3CN concentration for test solutions; (a) 1×10^{-5} M Al(III), (b) 1×10^{-5} M Ga(III) and (c) none containing 1×10^{-2} M Mo(VI) and 5×10^{-2} M monochloroacetate (pH 2.0). Measured after standing at room temperature for 20 min. Migration buffer; 1×10^{-1} M monochloroacetate (pH 2.0). Applied voltage; -13.0 kV.

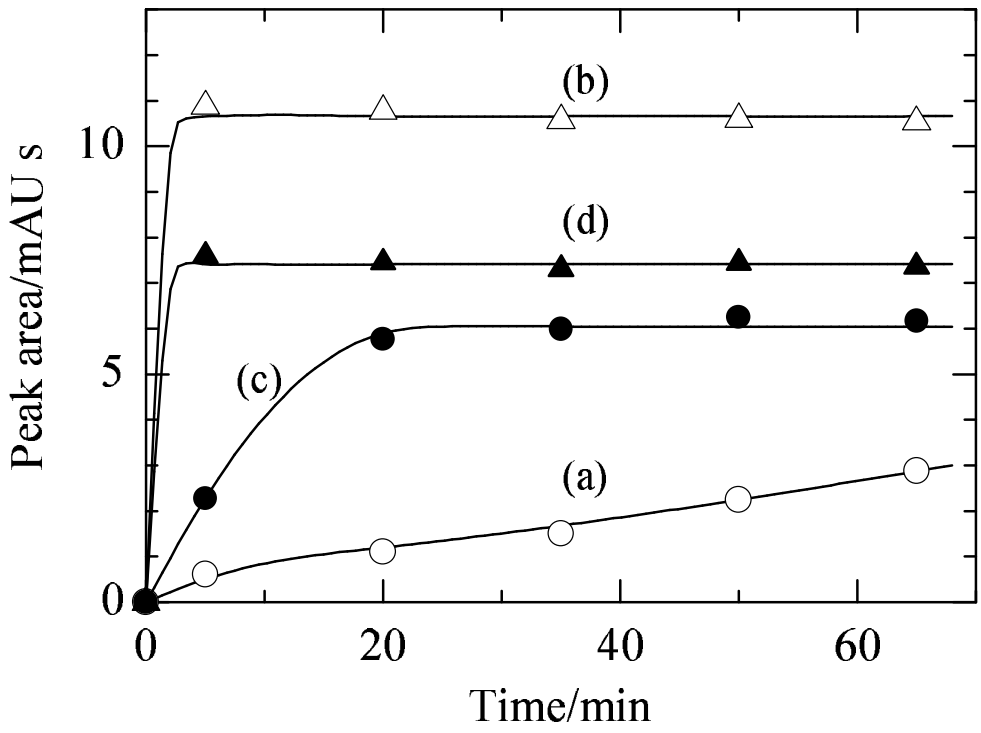

Figure 5.4: Peak area as a function of the reaction time for 1×10^{-3} M Mo(VI)–(a), (c); 1×10^{-5} M Al(III) and (b), (d); 1×10^{-5} M Ga(III)-5×10^{-2} M monochloroacetate (pH2.0) containing (c), (d); 60% (v/v) CH_3CN systems. Migration buffer; 0.1M monochloroacetate (pH 2.0). Applied voltage; −13.0 kV.

M) while keeping [Al(III)] or [Ga(III)]=1×10^{-5} M in 5×10^{-2} M monochloroacetate buffer (pH2.0) containing 60 % (v/v) CH_3CN. These solutions were introduced into the capillary, and electropherograms were recorded. In a series of electrophoretic measurements, 0.1 M monochloroacetate buffer (pH 2.0) was also used as a migration buffer.

As well as Chapter 2, in the all concentration ranges of Mo(VI), the peak due to the Al(III) and Ga(III) complexes are obtained, and above Mo(VI) concentrations 2×10^{-3} M, a few unknown peaks of isopolyoxomolybdates appears in the electropherograms. The result of these experiments were considered, the Mo(VI) concentration of 1×10^{-3} M was chosen as optimum.

5.3.2 Choice of the electrophoretic conditions

In establishing conditions for CE separations of heteropolyoxomolybdates, the following experiments were carried out. It was typical experiments that a test solution containing 1×10^{-5} M Al(III) and Ga(III), 1×10^{-3} M Mo(VI) and 5×10^{-2} M buffer (the same sort as the migration buffer) containing 60 % (v/v) CH_3CN.

The sort of buffer was diversified. At first, malonate, monochloroacetate, acetate, tartarate, and formate buffer solutions of pH 2.0–4.5 were examined to choose a proper migration buffer. Peaks were obtained for the each heteropolyoxomolybdate anions in all buffers without tartarate. With excepts of monochloroacetate buffers, they were less peak height or the interference from several isopolyoxomolybdate anion. Much better results were obtained only monochloroacetate

buffer over experimental pH ranges. In the each buffer, isopolymolybdate anions were not detected same migration time. This is because of the interaction between these complexes and the buffer components. The effect of the buffer has not been clarified, however, similar phenomena were described previously Chapters 2 and 3. The optimum concentration of migration buffer was found to be 0.1 M, cause a stability of baseline and peak separation between heteropolyoxo anions.

The effect of the pH of buffer on the electropherogram was investigated. The results obtained are summarized in Fig. 5.5 and 5.6, basis on the electropherograms containing 1×10^{-5} M analytes, 1×10^{-3} M Mo(VI) and 1×10^{-2} M monochloroacetate buffer. As shown in Fig. 5.5, the peaks due to the $[AlMo_6O_{24}H_6]^{3-}$ and $[GaMo_6O_{24}H_6]^{3-}$ were appeared at pH range of 1.8–4.0, but these peaks were overlapped at pH range up to 3.0. These pH ranges were consistent with formation ranges of these complexes that obtained through UV-Vis measurements. Figure 5.6 shows relationship between the migration time due to polyoxomolybdate complexes and pH values. In the pH range 1.8–3.0, both species showed well-separated. Although these ions have formed same charged complexes of Anderson structure, this electropherogram display well-shaped peaks. This simultaneous determination of Al(III) and Ga(III) is difficult by other determination methods.

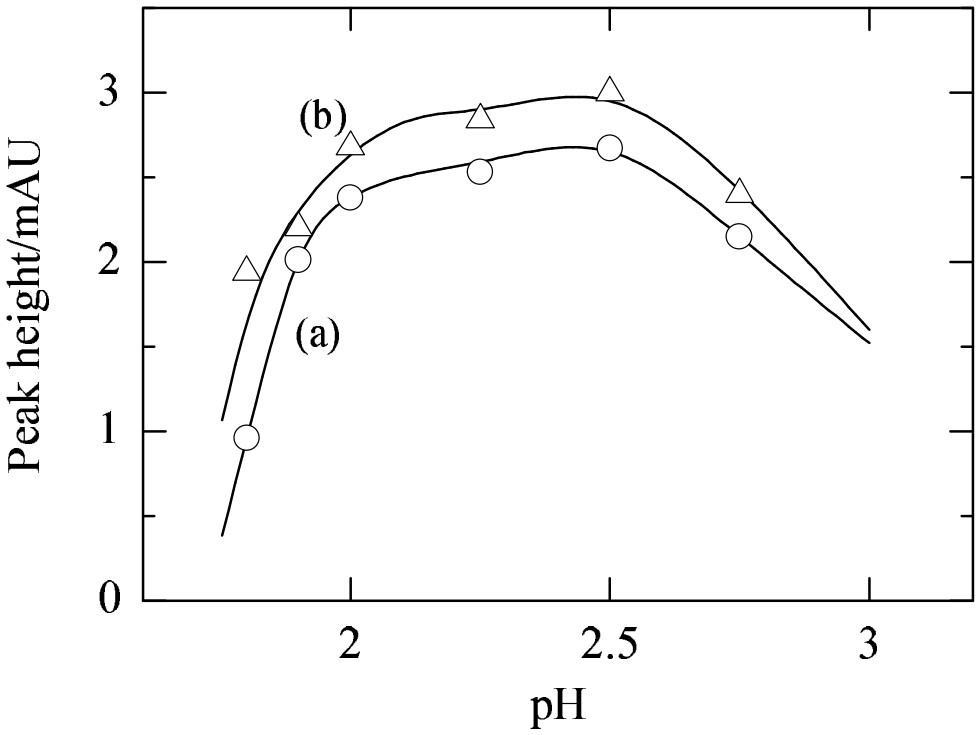

Figure 5.5: Peak height as a function of the pH value for test solutions; (a) 1×10^{-5} M Al(III) or (b) 1×10^{-5} M Ga(III), and 1×10^{-3} M Mo(VI) and 5×10^{-2} M monochloroacetate buffer containing 60% (v/v) CH_3CN systems. Migration buffer; 1×10^{-1} M monochloroacetate. Applied voltage; -13.0 kV.

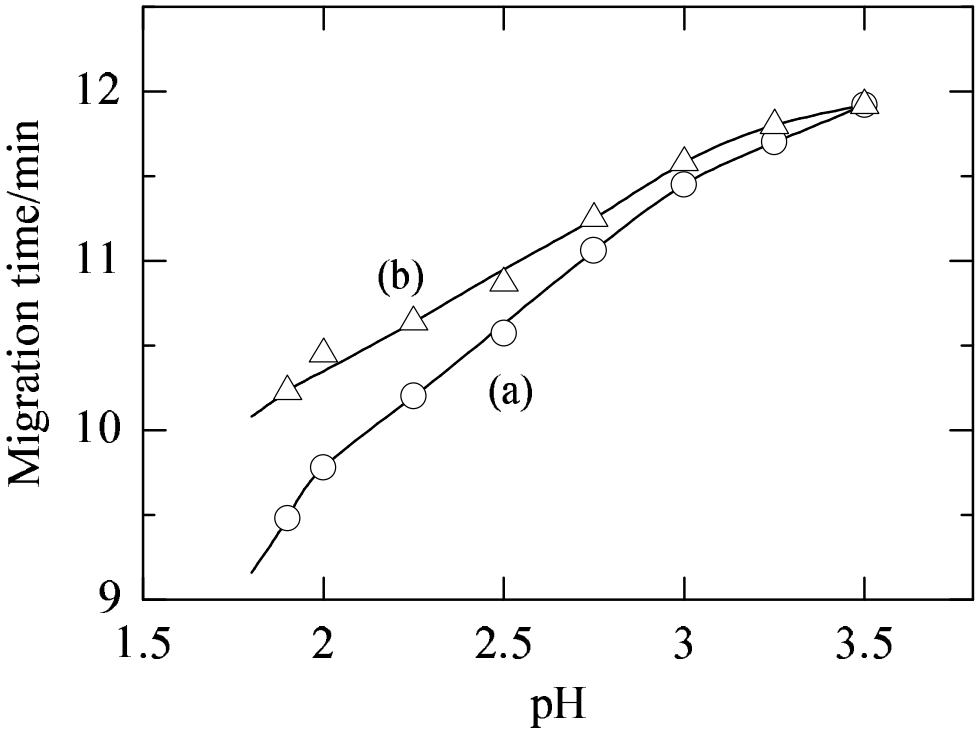

Figure 5.6: Migration time as a function of the pH value for test solutions; (a) 1×10^{-5} M Al(III) or (b) 1×10^{-5} M Ga(III), and 1×10^{-3} M Mo(VI) and 5×10^{-2} M monochloroacetate buffer containing 60% (v/v) CH_3CN systems. Migration buffer; 1×10^{-1} M monochloroacetate. Applied voltage; -13.0 kV.

5.3.3 The Conditions for the determination of Al(III) and Ga(III) ions

The capillary was filled with 0.1 M monochloroacetate (pH 2.0) before sample injection. A 1 mL portion of 1.0 M monochloroacetate buffer, which had same pH of migration buffer and a 0.2 mL of 0.1 M Mo(VI) were placed in a 20 mL volumetric flask. After the addition of an appropriate amount of an aqueous solution of Al(III) and Ga(III), 12 ml of CH_3CN was added. The solution was diluted to the mark with purified water. The electrophoretic analysis was made by introducing the sample solution into the capillary with hydrostatic injection for 30 s, and the difference in elevation was 25 mm. A voltage of −13.0 kV was applied for the separations. Direct UV detection was employed 240 nm, and the sampling rate was 0.5 s. At the same time, UV-visible spectra were measured at intervals of two nano meters. Throughout the experiments, the capillary was held in a thermostated cartridge controlled at 40°C. The migration times were recorded and calibration curves were obtained for analyte ions, respectively.

It was shown that the electropherogram of 1×10^{-5} M Al(III) and Ga(III) at optimum condition of pH 2.0 (Fig. 5.7). Al(III) and Ga(III), migration is this order. The electropherogram in Fig. 5.7 shows a very sharp, well-separated and reproducible peak for Al(III)- and Ga(III)-polyoxoanions, and a flat, smooth baseline. Determination errors of coexisting both Al(III) and Ga(III) were investigated on the variety concentration (Table 5.1 and 5.2). There are ignore errors on these studies with the exception of ten times concentration

of Ga(III) when determination of 1×10^{-5} M Al(III). The addition of ten times concentration of Al(III) also had no significant influence on determination of 1×10^{-5} M Ga(III).

5.3.4 Interference from foreign ions

The interference from several foreign ions was studied; the results are shown in Table 5.3. For determining Al(III) and Ga(III), phosphate and silicate ions caused negative errors by forming the corresponding a mixture of α- and β-Keggin-type heteropolyanions with Mo(VI), the formation of which lead to a lack of Mo(VI) as well as in Chapter 2. Cr(III) produced negative errors for the determination of Ga(III), because the peak of Cr(III)-complex overlaps to Ga(III).

5.3.5 Comparison of analytical performance

Figure 5.8 shows electropherograms of the detection of Al(III) and Ga(III) using indirect detection. Well-defined peaks can be observed in the electropherograms of indirect photometry using imidazole as background electrolytes each metal ions, but it could not provide complete separation of Al(III) and Ga(III). The peak which appears at a migration time of ca. 4.5 min can be assigned to the $Al(OH)_2^+$ since this species predominates in aqueous solution at pH ranges 3–5 (Fig. 5.8(a)). There is only one peak of Al(III) species on the electropherogram all over the concentration ranges. On the other hand, the peaks of Ga(III) species are appeared at migration time of ca. 1 and 4.5 min. Since the former peak area increase with decrease in pH, it is

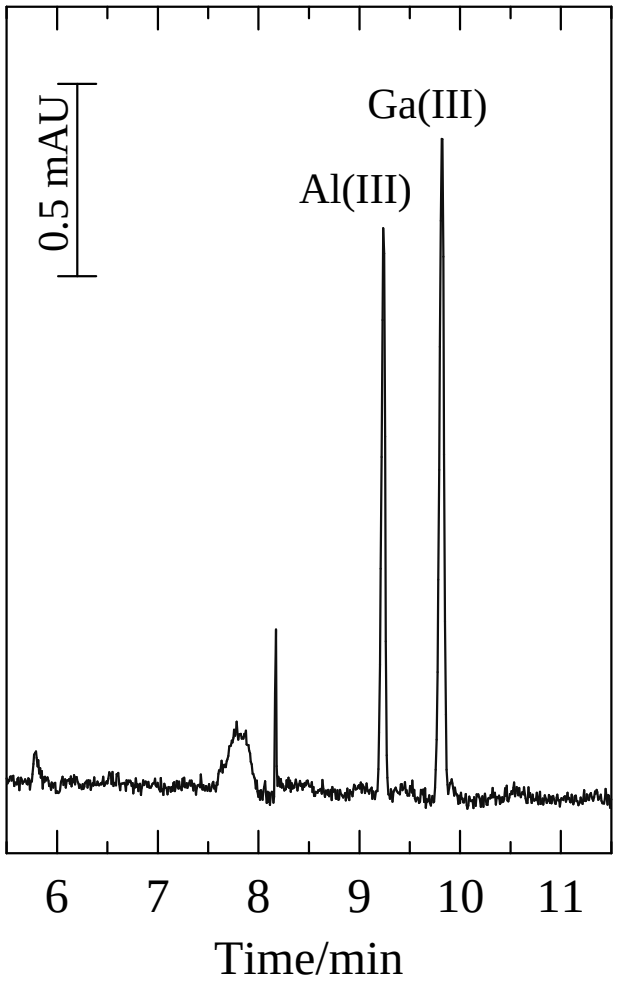

Figure 5.7: An electropherogram for a test solution; 1×10^{-5} M Al(III)–1×10^{-5} M Ga(III)–1×10^{-3} M Mo(VI)–5×10^{-2} M monochloroacetate buffer (pH 2.0) containing 60% (v/v) CH_3CN system. Migration buffer; 0.1M monochloroacetate (pH 2.0). Applied voltage; -12.0 kV.

Table 5.1: Effect of Ga(III) on the determination of 1×10^{-5} M Al(III).

[Ga(III)]/M	Relative error, %
5×10^{-6}	2.1
1×10^{-5}	−2.2
2×10^{-5}	1.5
5×10^{-5}	1.3
1×10^{-5}	−5.3

Sample: 1×10^{-3} M Mo(VI)–0.1 M monochloroacetate (pH 2.0) containing 60% (v/v) CH_3CN. Migration buffer: 0.1 M monochloroacetate (pH 2.0).

Table 5.2: Effect of Al(III) on the determination of 1×10^{-5} M Ga(III).

[Al(III)]/M	Relative error, %
5×10^{-6}	3.7
1×10^{-5}	−0.1
2×10^{-5}	0.8
5×10^{-5}	1.4
1×10^{-5}	1.4

Sample: 1×10^{-3} M Mo(VI)–0.1 M monochloroacetate (pH 2.0) containing 60% (v/v) CH_3CN. Migration buffer: 0.1 M monochloroacetate (pH 2.0).

Table 5.3: Effect of foreign ions on the determination of Al(III) and Ga(III).

Ions added as	Concentration/ M	Relative error, % Al(III)	Ga(III)
$NaIO_4$	1×10^{-4}	−4	−3
$Cr(NO_3)_3$	5×10^{-5}	−6	—
$FeCl_3$	1×10^{-4}	−2	−2
$NiSO_4$	1×10^{-4}	−3	4
$CuSO_4$	1×10^{-4}	1	−2
$Zn(NO_3)_2$	1×10^{-4}	−4	2
NaH_2PO_4	5×10^{-5}	−45	−48
Na_2SiO_3	1×10^{-4}	−17	−18
NaCl	1×10^{-2}	−5	−5

Sample: [Al(III)]=[Ga(III)]=1×10^{-5} M. 1×10^{-3} M Mo(VI)–5×10^{-2} M monochloroacetate (pH 2.0) containing 60% (v/v) CH_3CN. Migration buffer: 0.1 M monochloroacetate (pH 2.0).

assumed to migrate the naked Ga(III) ions, and the latter is similar to Al(III) species.

Minimum detectable concentration, linearity and reproducibility were examined under the above conditions. Table 5.4 and 5.5 show the detection limits and the determination ranges for these studies. The detection limit was 2×10^{-6} M for Al(III) and 5×10^{-7} M for Ga(III). This high detection limits are about 10 times greater than the value of above indirect photometric data, because of large optical density of heteropolyoxomolybdate anions. Correlation coefficients were 0.998 for Al(III) and 0.999 for Ga(III). The reproducibility was studied by making five consecutive runs of a standard solution at a concentration of 1×10^{-5} M of each hetero ions. The per cent relative standard deviation (RSD) is expressed as the quotient of the standard deviation and the mean value. The RSD of migration times for two complexes were less than 0.3%, although the RSD of peak areas for Al(III) and Ga(III) were less than 1.6% on these measurements.

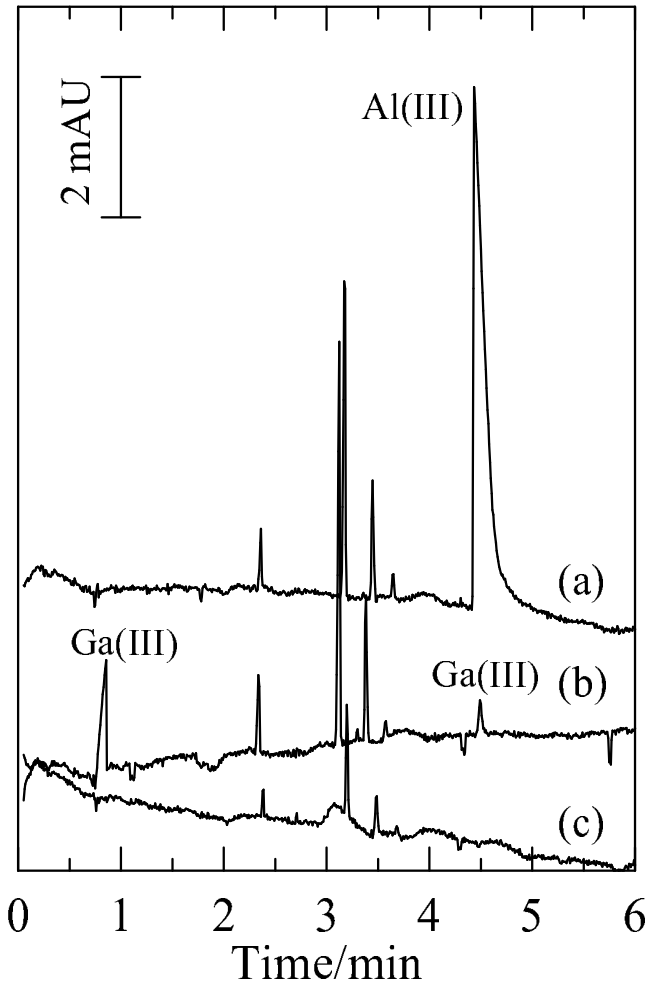

Figure 5.8: Electropherograms for test solutions containing (a) 5×10^{-4} M Al(III) and (b) 5×10^{-4} M Ga(III). Migration buffer; 5 mM imidazole (pH 4.0). Applied voltage; 22.0 kV.

Table 5.4: Concentration range and detection limits of Al(III).

Methods	Determination range/M	Detection limit/M
Heteropolyoxomolybdate	2×10^{-6}–1×10^{-4}	1×10^{-6}
Hydrostatic injection	1×10^{-5}–1×10^{-3}	5×10^{-6}
Electromigratic injection	1×10^{-6}–1×10^{-4}	5×10^{-7}

Table 5.5: Concentration range and detection limits of Ga(III).

Methods	Determination range/M	Detection limit/M
Heteropolyoxomolybdate	5×10^{-7}–1×10^{-4}	2×10^{-7}
Hydrostatic injection	5×10^{-5}–1×10^{-3}	2×10^{-5}
Electromigratic injection	5×10^{-6}–1×10^{-4}	2×10^{-6}

Chapter 6

Determination of P(V)

6.1 Introduction

In this Chapter, the author described the determination of P(V) based on the formation of dodecamolybdophosphate complex in an aqueous-organic solution.

Phosphate is one of the most restrictive nutrients and its analysis is of great importance in biological and environmental sciences. Several methods have been developed for the determination of P(V), including conventional colorimetry based on the formation of mixed-valence heteropoly blues (COL) [117], ion chromatography (IC) [118,119], flow injection analysis (FIA) [120], and capillary electrophoresis (CE) [53,54,57,121–128]. Recently, CE has shown to be a powerful technique for the analysis of P(V), in which the most common detection mode is indirect UV detection using suitable absorbing anions such as chromate [129]. Owing to a high background absorbance, however, the indirect detection method has the disadvantage of high noise, and is not sufficiently sensitive for the trace analysis of P(V).

Unlike anions, cations can be determined with direct UV detection after the complex-formation. With the exception of heteropolyoxometalates, on the other hand, there are few complexes incorporating anions, and direct UV detection is possible only for oxoanions that absorb in the UV region, as stated above.

Recently, remarkable progress in the preparation of polyoxometalate complexes has been made using water-miscible organic solvents like CH_3CN [109–116]. In the present study, we have found that a Keggin-type $[PMo_{12}O_{40}]^{3-}$ complex, which is unstable in aqueous solution, can be stabilized by the presence of CH_3CN as an auxiliary solvent. In such aqueous-CH_3CN solutions, the Keggin complex is formed at very low concentrations of Mo(VI) and P(V). On the basis of the complex-formation reaction, a simple and sensitive method was developed for the CE determination of P(V) with direct UV detection. The CE method offers the advantage of detecting P(V) with high sensitivity and eliminating interferences from sample matrices. The utility was demonstrated in the analysis of P(V) in river water.

6.2 Experimental

6.2.1 Apparatus

Apparatus of capillary electrophoresis and UV-visible spectroscopy system used were described in Chapter 4. For the IC measurement, a Dionex DX–300 system was used with a electrolytes suppressor and a conductivity detector. The separation column was a Dionex ICE–

AS1, and the eluent comprised 1.7 mM $NaHCO_3$ and 1.8 mM Na_2CO_3. The determination of P(V) by COL was carried out according to the literature method [117]. Voltammetric measurements were made with a Hokuto Denko HA–501 potentiostat interfaced to a microcomputer-controlled system. A glassy carbon electrode GC–30S (Tokai carbon) with a surface area of 7.1 mm^2 was used as a working electrode and a platinum wire served as the counter electrode. The reference electrode was an Ag/AgCl electrode. The voltammograms were recorded at 25±0.1°C. The voltage scan rate was set at 100 $mV \cdot s^{-1}$.

6.2.2 Reagents

The α-Keggin type $[PMo_{12}O_{40}]^{3-}$ complex was synthesized from the literature method [130]. All other reagents used were described in Chapter 4.

6.3 Results and Discussion

6.3.1 Formation of α- and β-dodecamolybdophosphate complexes in aqueous-CH_3CN media

The stability of the Keggin-type $[PMo_{12}O_{40}]^{3-}$ complex should be taken into account when the complex-formation reaction is applied to the CE analysis of P(V). In order to clarify the effect of CH_3CN on the stability of the Keggin complex, cyclic voltammograms were recorded for 1.0×10^{-5} M α-$[PMo_{12}O_{40}]^{3-}$ in 0.050 M HCl with and without 60% (v/v) CH_3CN. In the presence of 60% (v/v) CH_3CN, a

two-step redox wave was obtained and the wave shape was unchanged for at least two hours (Fig. 6.1(a)). In the absence of CH_3CN, on the other hand, the wave height was only half that shown in Fig. 6.1(a), being decreased as time passed. Consequently, the wave disappeared completely in three minutes (Fig. 6.1(c)). These results clearly show that the Keggin complex is stable only in the presence of CH_3CN.

Recently, the formation of the α-$[PMo_{12}O_{40}]^{3-}$ complex was ascertained in aqueous solutions of 100 mM Mo(VI) and 0.5 M HCl containing P(V) at concentrations < 7 mM [50]. In the presence of CH_3CN, the Keggin complex is formed at much lower concentrations of Mo(VI) and P(V). Figure 6.2 shows cyclic voltammograms for a 10.0 mM Mo(VI)–0.10 mM P(V)–0.050 M HCl–60% (v/v) CH_3CN system. As shown in Fig. 6.2(a), a well-defined three-step redox wave was obtained immediately after the preparation of the solution. As time elapsed, the first wave decreased with an increase of the third wave (Fig. 6.2(b)), indicating the spontaneous transformation of β-$[PMo_{12}O_{40}]^{3-}$ into the α-isomer [131]. The redox waves were numbered in the direction of more cathodic potentials. It should be stressed that the total concentrations of the α- and β-isomers are unchanged during the transformation. Then, the effect of the CH_3CN or HCl concentration on the formation of the Keggin complexes was investigated. The redox waves due to both Keggin complexes appeared in the 10 mM Mo(VI)–0.10 mM P(V)–0.050 M HCl system at CH_3CN concentrations $> 10\%$ (v/v), and increased in height with an increase of the CH_3CN concentration; two-liquid layers resulted at CH_3CN concentrations$> 80\%$ (v/v). The Keggin complexes were formed in

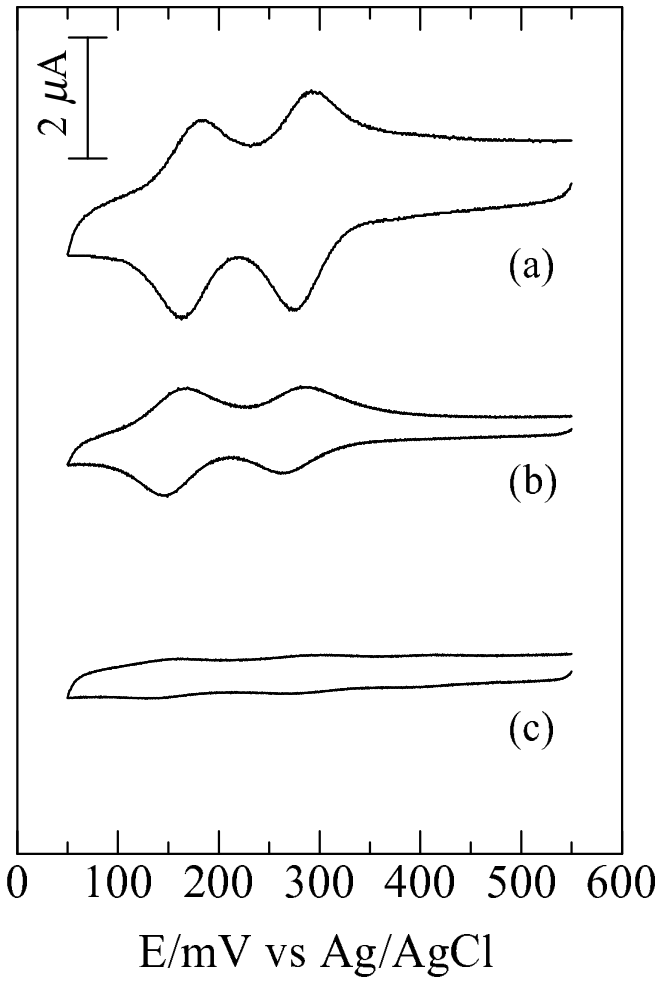

Figure 6.1: Cyclic voltammograms for 1.0×10^{-5} M α-$[PMo_{12}O_{40}]^{3-}$ in 0.050 M HCl; (a) with and (b), (c) without 60% (v/v) CH_3CN. Measured (a), (b) immediately after the preparation; (c) after 3 minutes.

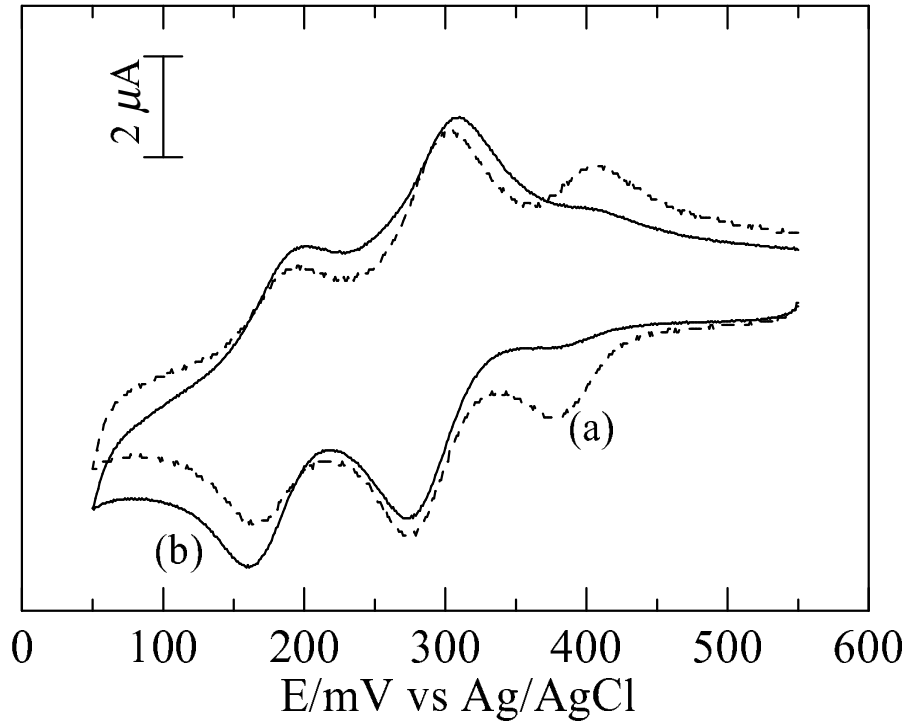

Figure 6.2: Cyclic voltammograms for a 10.0 mM Mo(VI)–0.10 mM P(V)–0.050 M HCl–60% (v/v) CH_3CN system. Measured (a) immediately after the preparation; (b) after 5 hours.

the HCl concentration range of 0.030–0.080 M, and the maximal reduction current was obtained at 0.050 M HCl.

6.3.2 Effect of the Mo(VI) concentration

In establishing conditions for CE measurements, test solutions were prepared by varying the Mo(VI) concentration (1–50 mM) while keeping [P(V)]=1.0x10-5 M, [HCl]=0.050 M, and [CH_3CN]=60% (v/v). In

a series of CE measurements, a 0.050 M HCl–60% (v/v) CH_3CN system was used as a migration electrolyte. In the Mo(VI) concentration range studied, a sharp peak due to the migration of the α- and β-isomers was obtained in the electropherogram. In agreement with the voltammetric results, the peak area was reproducible even when the test solution was introduced immediately after the preparation. At Mo(VI) concentrations > 5.0 mM, several peaks due to unknown isopolyoxomolybdates appeared and one of them caused serious interferences owing to the overlapping with the Keggin peak. Taking the voltammetric results into account, the 2.5 mM Mo(VI)–0.050 M HCl–60% (v/v) CH_3CN system was chosen as a compromise for the CE determination of P(V). The 0.050 M HCl–60% (v/v) CH_3CN system was found to be optimum as the migration electrolyte, because migration under these conditions gave the best sensitivity to detection. The absence of CH_3CN in the migration electrolyte caused the Keggin peak to disappear, owing to the decomposition of the Keggin complex.

6.3.3 Choice of acid

The choice of acid in sample solutions is effective on detection sensitivity. Figure 4.6 in chapter 4 shows electropherograms for a 2.5 mM Mo(VI)–5×10^{-6} M P(V)–60% (v/v) CH_3CN system containing 0.050 M of HCl, CF_3SO_3H, H_2SO_4, CH_3SO_3H or XSA. When XSA was used instead of HCl, the peak height was increased by approximately 3.5-fold, owing to the transitional isotachophoresis effect [89]. The direct detection developed in the present study gave a linear calibration

curve over the P(V) concentration range of 5×10^{-7}–5×10^{-5} M. The correlation coefficient was 0.997.

6.3.4 The CE procedure

The capillary was filled with 0.050 M HCl–60% (v/v) CH_3CN solution before sample injection. A 1 ml portion of 1 M XSA and a 1 ml of 50 mM Mo(VI) were placed in a 20 ml volumetric flask. After the addition of an appropriate amount of an aqueous solution of P(V), 12 ml of CH_3CN was added. The solution was diluted to the mark with purified water. The sample solution thus obtained was introduced into the capillary with hydrostatic injection for 60 s. The applied voltage of −8.5 kV was chosen as best, because the electropherogram showed a sharp peak with minimal migration time and a smooth baseline. Lower applied voltage increased the analysis time and broadened the peak. On the other hand, the base line became noisy at higher applied voltage, probably owing to the Joule heating effect. Throughout the experiments, the capillary was held in a thermostated cartridge controlled at 30°C. The Keggin peak was detected at 220 nm, and the amount of P(V) was determined from the calibration curve.

It is compared the two spectra on the Fig. 6.3 that UV spectrum of the peak bear striking resemblance to own heteropolyoxomolybdate anions. The 5×10^{-5} M $(Bu_4N)_3[PMo_{12}O_{40}]$ in neat CH_3CN was measured by capillary electrophoresis on the same condition. The migration time due to $(Bu_4N)_3[PMo_{12}O_{40}]$ in neat CH_3CN is almost consistent with the above procedure. Accordingly, the electrophoretic

species has been evidently dodecamolybdophosphate, which should not be decomposed in measurement.

6.3.5 Interference from foreign ions

In the optimized aqueous-CH_3CN solution, Mo(VI) can react with other oxoanions to form the corresponding polyoxomolybdate complexes, which may migrate in the capillary to cause serious interferences. Migration of polyoxomolybdate anions incorporating $P_2O_7^{4-}$, PHO_3^{2-}, VO_3^{-}, SiO_3^{2-}, GeO_3^{2-}, AsO_3^{3-}, and AsO_4^{3-} was investigated under the recommended conditions, and the results are shown in Table 6.1. With the exception of AsO_4^{3-}, these oxoanions caused only negligible interference since the peaks due to the polyoxomolybdate anions were well resolved. However, AsO_4^{3-} interfered with the determination of P(V) because peaks due to both Keggin-type $[AsMo_{12}O_{40}]^{3-}$ and $[PMo_{12}O_{40}]^{3-}$ complexes were overlapped. The presence of NaCl in concentrations up to 1×10^{-2} M did not interfere.

6.3.6 Analysis of P(V) in river water

The developed CE method was applied to the determination of P(V) in river water. The sample water from the Yamato River was stored in a polyethylene bottle at 4°C, and filtrated on a 0.45 μm membrane filter before analysis (Fig. 6.3). As shown in Table 6.2, the peak areas due to the $[PMo_{12}O_{40}]^{3-}$ anion were satisfactorily reproducible with a R.S.D. value (n=5) of 0.2%, and the CE results agreed well with the IC results.

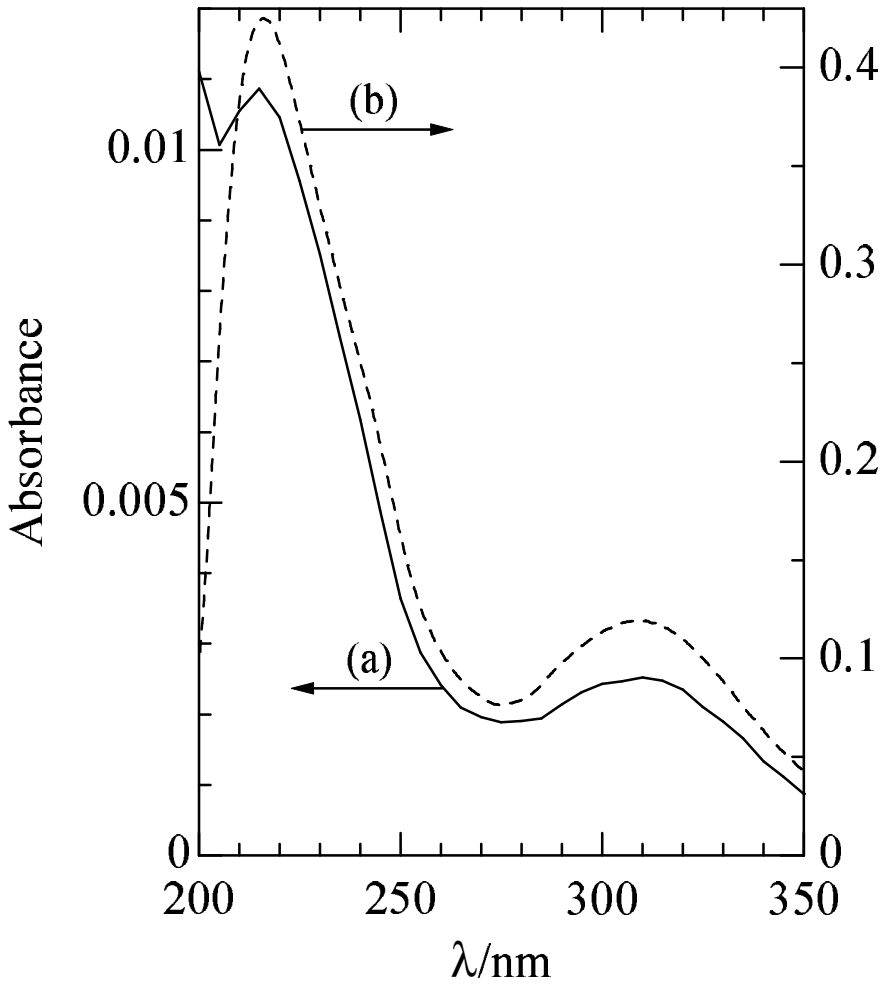

Figure 6.3: Absorption spectra for (a) the peak of phosphate complex in Fig. 4.6(e), and (b) 5×10^{-5} M solution of $(Bu_4N)_3[PMo_{12}O_{40}]$ in neat CH_3CN, path length, 1 mm.

Table 6.1: Effect of foreign ions on the determination of phosphate.

Ions added as	Conc./M	Relative error, %
NaCl	1×10^{-1}	−22
	5×10^{-2}	−10
	1×10^{-2}	−4
$Na_4P_2O_7$	1×10^{-4}	1
Na_2PHO	1×10^{-4}	−1
NH_4VO_3	1×10^{-4}	−3
Na_2SiO_3	1×10^{-4}	2
Na_2GeO_3	1×10^{-4}	3
Na_2HAsO_4	1×10^{-5}	36
Na_3AsO_3	1×10^{-4}	5

Test solution; 1×10^{-5} M phosphate–2.5 mM Mo(VI)–50 mM XSA–60%(v/v) CH3CN. Migration buffer; 50 mM HCl–60%(v/v) CH3CN. Applied voltage; −8.5 kV.

Table 6.2: A comparison of the results obtained with COL, IC and CE method

Methods	Determination range/M	Detection limit/M	River water Found/ppm	River water RSD[a],%
CE	5×10^{-7}–5×10^{-5}	1×10^{-7}	1.39 ± 0.08	2.0
Indirect-CE[b]	5×10^{-6}–5×10^{-4}	1×10^{-6}	1.32 ± 0.23	5.9
IC	5×10^{-6}–5×10^{-4}	1×10^{-6}	1.22 ± 0.18	4.9
COL	5×10^{-7}–5×10^{-5}	1×10^{-7}	1.33 ± 0.02	0.5

[a]Values obtained in 5 measurements.
[b]Migration buffer; 3 mM K_2CrO_4–0.2 mM TTAB–10 mM borate (pH 8.5). Applied voltage; −15.0 kV.
[c]Path length; 25 mm.

Comparison with COL showed that the present CE method had a comparable sensitivity and a better reproducibility (Table 6.2). The detection limits for CE and COL are similar and lower than those for IC. However, COL is not specific for phosphate, and a combination with some separation technique is needed.

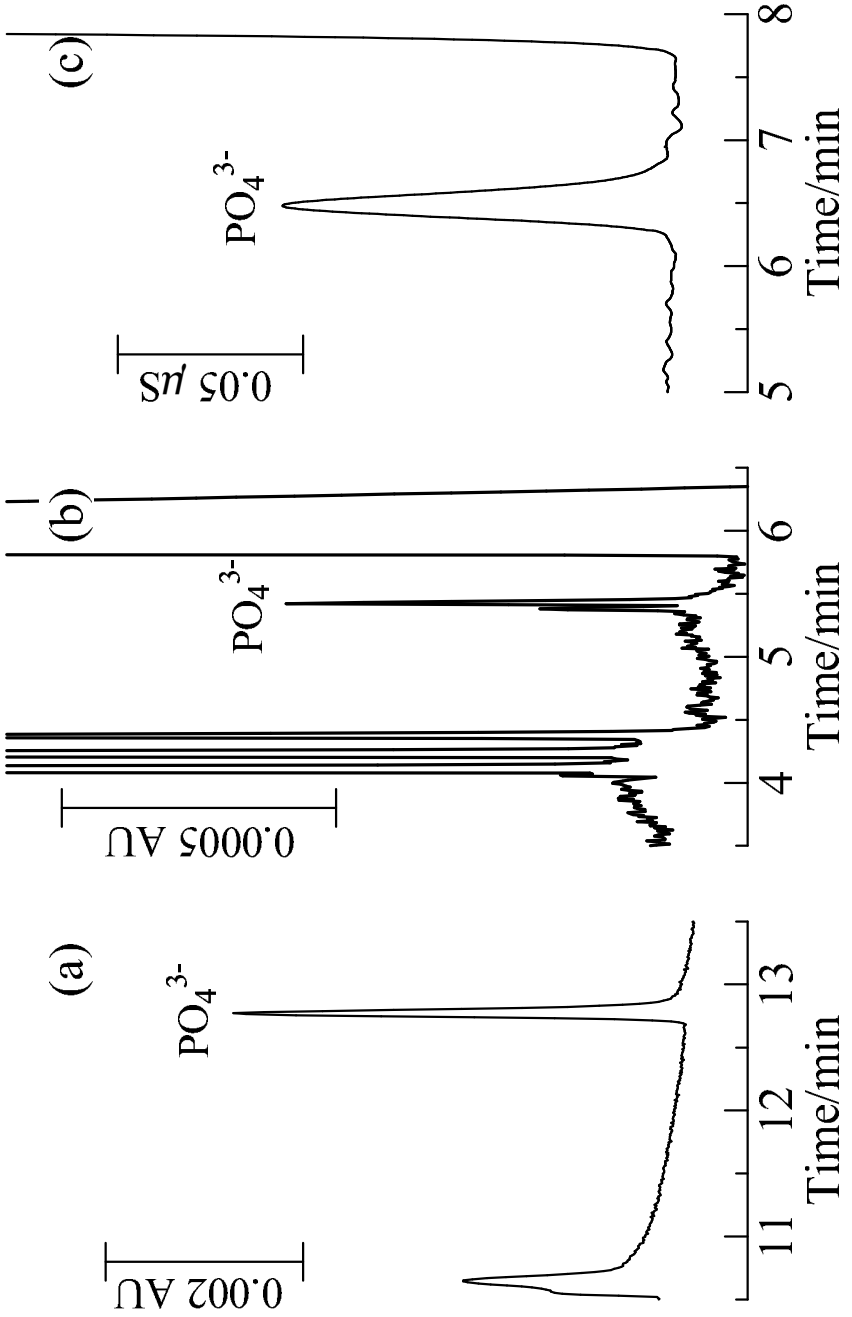

Figure 6.4: An analysis of river water by (a) CE, (b) indirect CE and (c) IC.

Conclusion

In this study, the author has proposed novel analytical methods based on the formation of heteropolyoxomolybdates by mean of capillary electrophoresis.

In Chapter 2, the simultaneous CE determination of Cr(III) and Cr(VI) has been studied, which is a simple and sensitive method by mean of the capillary electrophoretic analysis. In a 0.1 M monochloroacetate buffer of pH 2–3, Mo(VI) reacts rapidly, even at room temperature with Cr(III), to form a stable heteropoly anion. Both anionic forms of Cr(III) and Cr(VI) can be determined simultaneously by capillary electrophoresis with UV detection at 256 nm. Linear calibration curves were obtained in the concentration ranges of 5×10^{-6}–1×10^{-4} M and 1×10^{-5}–1×10^{-4} M for Cr(III) and Cr(VI), respectively; the detection limits were 2×10^{-6} and 5×10^{-6} M. The author has also described the interference from foreign ions.

In Chapter 3, the author has described the simultaneous CE determination of I(VII) and I(V). In a 5×10^{-2} M malonate buffer solution (pH 4) containing low concentrations of I(VII) and 1×10^{-2} M Mo(VI), a stable $[IMo_6O_{24}]^{5-}$ complex was formed at room temperature. Since the heteropoly anion showed an approximately eight-fold

increase in the molar absorption coefficient than the free IO_4^- anion, the complex-formation reaction was applied to the sensitive capillary electrophoretic determination of I(VII) with UV detection at 220 nm. Simultaneous determination of I(VII) and I(V) was also possible since both peaks due to $[IMo_6O_{24}]^{5-}$ and IO_3^- were well-separated in the electropherogram. For I(VII) and I(V), linear calibration curves were obtained in the concentration ranges of 2×10^{-6}–2×10^{-4} M and 5×10^{-5}–2×10^{-3} M, respectively.

In Chapter 4, the stacking effect on CE analysis based on the formation of heteropolyoxometalate has been investigated to improve separation efficiency and detection limit. The isomers of a Keggin-type dodecamolybdosilicate with approximately the same migration time could be separated satisfactorily by the normal sample stacking or the transitional isotachophoretic stacking. Similarly, the migration peaks due to the Anderson-type complexes became sensitive, so that the very sensitive determination of Cr(III) was also possible. Furthermore, the transitional isotachophoretic stacking was effective on the determination of phosphate based on the formation of a Keggin-type complex in aqueous-CH_3CN media.

In Chapter 5, the simultaneous CE determination of Al(III) and Ga(III) has been studied. The author has found that $[AlMo_6O_{24}H_6]^{3-}$ being formed slowly in aqueous solution, is immediately formed by the presence of water-miscible organic solvents like CH_3CN as auxiliary solvents. Ga(III) also reacts with Mo(VI) under the same condition of Al(III). These complexes with approximately the same migration time could be separated satisfactorily by the normal sample stacking

or the transitional isotachophoretic stacking as well as a Keggin-type dodecamolybdosilicate. On the basis of these findings, the migration peaks due to the Anderson-type complexes became sensitive and well separated, so that the simultaneous determination of Ga(III) and Al(III) was also possible. Linear calibration curves of both complexes were obtained in the concentration ranges of 2×10^{-6}–1×10^{-4} M and 5×10^{-7}–1×10^{-4} M for Al(III) and Ga(III), respectively; the detection limits were 1×10^{-6} and 2×10^{-7} M.

In Chapter 6, a sensitive method has been developed for the capillary electrophoretic determination of phosphate. In a 2.5 mM Mo(VI)–0.050 M *p*-$C_6H_3(CH_3)_2$-2-SO_3H (XSA)–60% (v/v) CH_3CN system, a trace of phosphate immediately formed a mixture of α- and β-Keggin type $[PMo_{12}O_{40}]^{3-}$ complexes, the total amount of which was directly proportional to the P(V) concentration. Since the Keggin complexes possessed high molar absorptivities, a capillary electrophoretic method with direct UV detection was developed for the determination of phosphate; the Keggin species was monitored at 220 nm. A 0.050 M HCl–60% (v/v) CH_3CN system was used as the migration electrolyte. The peak area was linearly dependent on the phosphate concentration in the range of 5×10^{-7}–5×10^{-5} M; a detection limit of 1×10^{-7} M was achieved. In comparison with indirect UV detection, the direct UV detection is about ten times more sensitive. The developed CE method was applied to the determination of phosphate in river water, and the results were in good agreement with those obtained by ion chromatography and colorimetry based on the formation of mixed-valence heteropoly blue species.

The author has demonstrated that heteropolyoxomolybdates which have many chemical equilibria in the solution can be separated one another by mean of capillary electrophoresis. These methods have been able to avoid the interference of coexistent species at the detection of the analytes, and so this article has hold out the hope that novel analytical method would be developed from the viewpoint of ‘speciation’.

Acknowledgment

The author is thankful to Dr. Sadayuki Himeno, Professor of Kobe University, for his helpful direction and suggestion fertile in science, and he expresses an appreciation for his gracious guidance and encouragement throughout the course of this study. He is also grateful to the Technology Research Institute of Osaka Prefecture and the members of there, specially Mr. Takeshi Tanimura (Deputy Director General), Mr. Ryosuke Nogami (Head of Evaluation Technology Dept.), Dr. Syozo Tamaki, Dr. Takumi Sone, Mr. Katsumi Inoue, Mr. Yoshio Sakai, Dr. Kiyoshi Yamasaki, Mr. Masahiro Mori, Mr. Yoshihiro Yobiko, Dr. Mitsuru Tahara, Dr. Hitoshi Morita and Mr. Shigeo Nozawa, for supporting his studies. He is indebted to Ms. Hui Shen, Mr. Kohji Kusuyama and Mr. Takuya Goto for their heartfelt assistance in accomplishment long and serviceable experiments as well. Finally, he wishes to thank for numerous experimental supports to Dr. Nobuhiro Ishio (Kobe University of Mercantile Marine), Mr. Masashi Hashimoto, Mr. Hirotaka Niiya, Mr. Ken-ichi Sano, Ms. Mayumi Yoshihara, Ms. Masayo Takamoto, Mr. Iwao Kitazumi, Mr. Hitoshi Nishikawa, Mr. Hideki Tatewaki, Ms. Ayumi Higuchi, Ms. Reiko Kuzuoka, Mr. Soichi Imanaka and Mr. Koichiro Hiwa.

References

[1] M. Bernhardt, F.E. Brinkman, P.J. Sadler (Eds.), "The importance of Chemical 'Speciation' in Environmental Processes", Springer-Verlag, Berlin (1986).

[2] E. Nieboer, *Analyst* **117** (1992) 550.

[3] M.G. van den Berg, *Anal. Chimi. Acta* **284** (1994) 461.

[4] J.W. Jorgenson, K.D. Lukacs, *Anal. Chem.* **53** (1981) 1298.

[5] P.L.St. Claire, III, *Anal. Chem.* **68** (1996) 569R.

[6] W.G. Kuhr, C.A. Monnig, *Anal. Chem.* **64** (1992) 389R.

[7] W.G. Kuhr, *Anal. Chem.* **62** (1990) 403R.

[8] D.R. Baker, "Capillary Electrophoresis", John Wiley & Sons, Inc., New York (1995).

[9] E. Dabek-Zlotozynska, E.P.C. Lai, A.R. Timerbaev, *Anal. Chim. Acta* **359** (1998) 1.

[10] K.L. Rundlett, D.W. Armstrong, *J. Chromatogr. A* **721** (1996) 173.

[11] P. Doble, P.R. Haddad, *J. Chromatogr. A* **834** (1999) 189.

[12] A. Padarauskas, G. Schwedt, *J. Chromatogr. A* **773** (1997) 351.

[13] J. Xu, P. Che, Y. Ma, *J. Chromatogr. A* **749** (1996) 287.

[14] T. Takayanagi, E. Wada, S. Motomizu, *Anal. Chem.* **12** (1996) 575.

[15] P. Janoš, *J. Chromatogr. A* **834** (1999) 3.

[16] M.T. Pope, "Heteropoly and Isopoly Oxometalates", Springer-Verlag, Berline (1983).

[17] D.E. Katsoulis, *Chem. Rev.* **98** (1998) 359.

[18] K. Matsuo, K. Urabe, Y. Izumi, Chem. Lett. (1981) 1315.

[19] M.L. Bianchi, R. Crisol, U. Schuchardt, *Bioresource Technology* **68** (1999) 17.

[20] S. Himeno, K. Kusuyama, M. Hashimoto, N. Ishio, *Anal. Sci.* **14** (1998) 681.

[21] S. Himeno, T. Ueda, H. Niiya, I. Iwai, T. Hori, *Anal. Sci.* **13** (1997) 369.

[22] K. Hettiarachchi, Y. Ha, T. Tran, A.P. Cheung, *J. Pharmaceutical & Biomedical Analysis* **13** (1995) 515.

[23] J. Kotaś, Z. Stasicka, *Environmental Pollution* **107** (2000) 263.

[24] B.E. Saltzman, *Anal. Chem.* **24** (1952) 1016.

[25] T.L. Alien, *Anal. Chem.* **30** (1958) 447.

[26] M. Martinez, M. Aguilar, *J. Chromatogr.* **676** (1994) 443.

[27] M.J. Thornton, J.S. Fritz, *J. Chromatogr.* **770** (1997) 301.

[28] D.T. Gjerde, D.R. Wiederin, F.G. Smith, B.M. Mattson, *J. Chromatogr.* **640** (1993) 73.

[29] J. Prokisch, B. Kovacs, Z. Gyori, J. Loch, *J. Chromatogr.* **683** (1994) 253.

[30] Y. Suzuki, *J. Chromatogr.* **415** (1987) 317.

[31] T. Williams, P. Jones, L. Ebdon, *J. Chromatogr.* **482** (1989) 361.

[32] G.Y. Jung, Y.S. Kim, H.B. Lim, *Anal. Sci.* **13** (1997) 463.

[33] A.R. Timerbaev, O.P. Semenova, W. Buchberger, G.K. Bonn, *J. Analyt. Chem.* **354** (1996) 414.

[34] S. Pozdniakova, A. Padarauskas, *Analyst* **123** (1998) 1497.

[35] L.C.W. Baker, G. Foster, W. Tan, F. Scholnick, T.P. McCutcheon, *J. Am. Chem. Soc.* **77** (1955) 2136.

[36] A. Perloff, *Inorg. Chem.* **9** (1970) 2228.

[37] O. W. Rollins, *J. Inorg. Nucl. Chem.* **33** (1971) 75.

[38] K. Nomiya, T. Takahashi, T. Shirai, M. Miwa, *Polyhedron* **6** (1987) 213.

[39] S. Himeno, H. Niiya, T. Ueda, *Bull. Chem. Soc. Jpn.* **70** (1997) 631.

[40] J.S. Dixon, D. Lipkin, *Anal. Chem.* **26** (1954) 1092.

[41] A.K. Hareez, W.A. Bashir, *Microchem. J.* **31** (1985) 375.

[42] J.J.B. Nevado, P.V. Gonzalez, *Analyst[London]* **114** (1989) 989.

[43] R.H. Coe, L.B. Rogers, *J. Am. Chem. Soc.* **70** (1948) 3276.

[44] P. Souchay, *Anal. Chim. Acta* **2** (1948) 17.

[45] S. Honda, S. Sudo, K. Kakehi, K. Takiura, *Anal. Chim. Acta* **77** (1975) 274.

[46] J. Palomares, A. Travesi, G. Dominguez, *Radiochem. Radioanal. Lett.* **3** (1970) 357.

[47] S. Honda, K. Suzuki, K. Kakehi, *Anal. Biochem.* **177** (1989) 62.

[48] B. Gruttner, G. Jander "Handbook of Preparative Inorganic Chemistry", ed. G. Brauer, Vol. 2, p. 1738, Academic Press, New York, 1965.

[49] M. Filowitz, R. K. C. Ho, W. G. Klemperer, W. Shum, *Inorg. Chem.* **18** (1979) 93.

[50] S. Himeno, M. Hashimoto, T. Ueda, *Inorg. Chim. Acta* **284** (1999) 237.

[51] J.D.H. Strickland, *J. Am. Chem. Soc.* **74** (1952) 862.

[52] J.D.H. Strickland, *J. Am. Chem. Soc.* **74** (1952) 868.

[53] J.J. Corr, J.F. Anacleto, *Anal. Chem.* **68** (1996) 2155.

[54] H. Liu, P.K. Dasgupta, *Anal. Chem.* **69** (1997) 1211.

[55] P.K. Jensen, C.S. Lee, J.A. King, *Anal. Chem.* **70** (1998) 730.

[56] X. Huang, R.N. Zare, S. Sloss, A.G. Ewing, *Anal. Chem.* **63** (1991) 189.

[57] D. Kaniansky, V. Zelenská, D. Baluchová, *Electrophoresis* **17** (1996) 1890.

[58] R.A. Wallingford A.G. Ewing, *Anal. Chem.* **59** (1987) 1762.

[59] R.A. Wallingford A.G. Ewing, *Anal. Chem.* **61** (1989) 98.

[60] L.A. Colón, R. Dadoo, R.N. Zare, *Anal. Chem.* **65** (1993) 948.

[61] T.J. O'Shea, S.M. Lunte, W.R. LaCourse, *Anal. Chem.* **65** (1993) 948.

[62] W. Lu, R.M. Cassidy, *Anal. Chem.* **65** (1993) 2878.

[63] J. Wen, A. Baranski, R. Cassidy, *Anal. Chem.* **70** (1998) 2504.

[64] T. Kappes, P.C. Hauser, *J. Chromatogr. A* **834** (1999) 89.

[65] F.E.P. Mikkers, F.M. Everaerts, Th.P.E.M. Verheggen, *J. Chromatogr.* **169** (1979) 11.

[66] F.E.P. Mikkers, F.M. Everaerts, Th.P.E.M. Verheggen, *J. Chromatogr.* **169** (1979) 1.

[67] F.M. Everaerts, Th.P.E.M. Verheggen, F.E.P. Mikkers, *J. Chromatogr.* **169** (1979) 21.

[68] Z.K. Shihabi, *J. Chromatogr. A* **902** (2000) 107.

[69] J.P. Quirino, S. Terabe, *J. Chromatogr. A* **902** (2000) 119.

[70] D.S. Burgi, *Anal. Chem.* **65** (1993) 3726.

[71] D.S. Burgi, R.L. Chien, *Anal. Chem.* **63** (1991) 2042.

[72] R.L. Chien, D.S. Burgi, *Anal. Chem.* **64** (1991) 489A.

[73] R.L. Chien, D.S. Burgi, *J. Chromatogr.* **559** (1991) 141.

[74] R.L. Chien, J.C. Helmer, *Anal. Chem.* **63** (1991) 1354.

[75] D.S. Stegehuis, H. Irth, U.R. Tjaden, J. van der Greef, *J. Chromatogr.* **538** (1991) 393.

[76] Z.K. Shihabi, *J. Chromatogr. A* **744** (1996) 231.

[77] Z.K. Shihabi, M. Friedberg, *J. Chromatogr. A* **807** (1998) 129.

[78] K. Sarmini, E. Kenndler, *J. Chromatogr. A* **833** (1999) 245.

[79] Z.K. Shihabi, *J. Chromatogr. A* **817** (1998) 25.

[80] M. Friedberg, M. Hinsdale, Z.K. Shihabi, *J. Chromatogr. A* **781** (1997) 35.

[81] W.F. Smyth, G.B. Harland, S. McClean, G. McGrath, D. Oxspring, *J. Chromatogr. A* **772** (1997) 161.

[82] M. Albert, L. Debusschere, C. Demesmay, J.L. Rocca, *J. Chromatogr. A* **757** (1997) 281.

[83] M. Albert, L. Debusschere, C. Demesmay, J.L. Rocca, *J. Chromatogr. A* **757** (1997) 291.

[84] J.P. Quirino, S. Terabe, *J. Chromatogr. A* **850** (1999) 339.

[85] Z. Krivácsy, A. Gelencsér, J. Hlavay, G. Kiss, Z. Sárvári, *J. Chromatogr. A* **834** (1999) 21.

[86] P.E. Jackson, P.R. Haddad, *J. Chromatogr.* **640** (1996) 481.

[87] A.M. Carro-Díaz, R.A. Lorenzo-Ferreira, R. Cela-Torrijos, *J. Chromatogr. A* **730** (1996) 345.

[88] C.X. Zhang, W. Thormann, *Anal. Chem.* **68** (1996) 2523.

[89] J. Boden, K. Bächmann, *J. Chromatogr. A* **734** (1996) 319.

[90] F. Kohlraush, *Ann. Phys. Chem. N.F.* **62** (1897) 209.

[91] K. Fukushi, K. Tada, S. Takeda, S. Wakida, M. Yamane, K. Higashi, K. Hiiro, *J. Chromatogr. A* **838** (1999) 303.

[92] L. Křivánková, A. Vraná, P. Gebauer, P. Boček, *J. Chromatogr. A* **772** (1997) 283.

[93] M. Danková, D. Kaniansky, S. Fanali, F. Iványi, *J. Chromatogr. A* **838** (1999) 31.

[94] V. Šustáček, F. Foret, P. Boček, *J. Chromatogr.* **545** (1991) 239.

[95] V. Pacáková, P. Coufal, K. Štulík, *J. Chromatogr. A* **834** (1999) 257.

[96] M. Chiari, *J. Chromatogr. A* **805** (1998) 1.

[97] S. Conradi, C. Vogt, H. Wittrisch, G. Knobloch, G. Werner, *J. Chromatogr. A* **654** (1996) 103.

[98] T.-I. Lin, Y.-H. Lee, Y.-C. Chen, *J. Chromatogr.* **654** (1993) 167.

[99] Y.-H. Lee, T.-I. Lin, *J. Chromatogr. A* **675** (1994) 227.

[100] C. François, Ph. Morin, M. Dreux, *J. Chromatogr. A* **717** (1995) 393.

[101] A.R. Timerbaev, W. Buchberger, O.P. Semenova, G.K. Bonn, *J. Chromatogr.* **630** (1993) 379.

[102] P. Kubáň, P. Kubáň, V. Kubáň, *J. Chromatogr. A* **836** (1999) 75.

[103] M. Blanco, J. Coello, F. González, H. Iturriaga, S. Maspoch, A.R. Puigdomènech, *Talanta* **43** (1996) 1489.

[104] S. Yamada, N. Ohta, M. Nakamura, S. Nakamura, *BUNSEKI KAGAKU* **41** (1992) 257.

[105] K. Yamamoto, H. Sunada, Y. Yonezawa, A. Otsuka, *BUNSEKI KAGAKU* **40** (1991) 495.

[106] H. Yamada, Y. Taguchi, H. Wada, *Anal. Sci.* **13** (1997) 355.

[107] Q. Wang, K. Tsunoda, H. Akaiwa, M. Sugiya, T. Watanabe, *Anal. Sci.* **12** (1996) 931.

[108] N. Wu, W.J. Horvath, P. Sun, C.W. Huie, *J. Chromatogr.* **635** (1993) 307.

[109] S. Himeno, T. Hori, A. Saito, *Bull. Chem. Soc. Jpn.* **62** (1989) 2184.

[110] S. Himeno, A. Saito, T. Hori, *Bull. Chem. Soc. Jpn.* **63** (1990) 1602.

[111] S. Himeno, T. Hori, A. Saito, *Bull. Chem. Soc. Jpn.* **64** (1991) 21.

[112] S. Himeno, T. Kubo, A. Saito, T. Hori, *Inorg. Chim. Acta* **236** (1995) 167.

[113] K. Maeda, S. Himeno, A. Saito, T. Hori, *Bull. Chem. Soc. Jpn.* **66** (1993) 1693.

[114] S. Himeno, K. Sano, H. Niiya, Y. Yamazaki, T. Ueda, T. Hori, *Inorg. Chim. Acta* **281** (1998) 214.

[115] S. Himeno, M. Takamoto, T. Ueda, *J. Electroanal. Chem.* **465** (1999) 129.

[116] S. Himeno, M. Yoshihara, M. Maekawa, *Inorg. Chim. Acta* **298** (2000) 165.

[117] J. Murphy, J.P. Riley, *Anal. Chim. Acta* **27** (1962) 31.

[118] F.S. Stover, J.A. Bulmahn, J.K. Gard, *J. Chromatogr. A* **688** (1994) 89.

[119] B. López-Ruiz, *J. Chromatogr. A* **881** (2000) 607.

[120] C.X. Galhardo, J.C. Masini, *Anal. Chim. Acta* **417** (2000) 191.

[121] F.S. Stover, *J. Chromatogr. A* **834** (1999) 243.

[122] T. Wang, S.F.Y. Li, *J. Chromatogr. A* **834** (1999) 233.

[123] D. Kaniansky, M. Masár, J. Marák, R. Bodor, *J. Chromatogr. A* **834** (1999) 133.

[124] K. Fukushi, S. Takeda, K. Chayama, S. Wakida, *J. Chromatogr. A* **834** (1999) 349.

[125] S.M. Valsecchi, S. Polesello, *J. Chromatogr. A* **834** (1999) 363.

[126] M.C.B. Alonso, R. Prego, *Anal. Chim. Acta* **416** (2000) 21.

[127] M. Panstar-Kallio, P.K.G. Manninen, *Chemosphere* **31** (1995) 3699.

[128] M.A. van den Hoop, J.J. van Staden, *J. Chromatogr. A* **770** (1997) 321.

[129] F. Foret, S. Fanali, L. Ossicini, P. Boček, *J. Chromartogr.* **470** (1989) 299.

[130] C. Rocchiccioli-Deltcheff, M. Fournier, R. Franck, R. Thouvenot, *Inorg. Chem.* **22** (1983) 207.

[131] S. Himeno, T. Osakai, A. Saito, *Bull. Chem. Soc. Jpn.* **62** (1989) 1335.

List for Publication

a) S. Himeno, Y. Nakashima, K. Sano, "Simultaneous Determination of Chromium(VI) and Chromium(III) by Capillary Electrophoresis", *Anal. Sci.* **14** (1998) 369.

b) Y. Nakashima, H. Shen, K. Kusuyama, S. Himeno, "Simultaneous Determination of Periodate(VII) and Iodate(V) by Capillary Electrophoresis", *Anal. Sci.* **15** (1999) 725.

c) Y. Nakashima, T. Goto, I. Kitazumi, S. Himeno, "Capillary electrophoretic determination of phosphate based on the formation of a Keggin-type $[PMo_{12}O_{40}]^{3-}$ complex", *Electrophoresis*, to be submitted.

d) Y. Nakashima, T. Goto, H. Shen, S. Himeno, "Simultaneous determination of Aluminum(III) and Gallium(III) based on the formation of the hexamolybdoalumate(III) and hexamolybdogallate(III)", in preparation.